

A review of hepatic nanotoxicology - summation of recent findings and considerations for the next generation of study designs

Kermanizadeh, Ali; Powell, Leagh G; Stone, Vicki

Journal of toxicology and environmental health. Part B, Critical reviews

DOI:

[10.1080/10937404.2020.1751756](https://doi.org/10.1080/10937404.2020.1751756)

Published: 18/05/2020

Publisher's PDF, also known as Version of record

[Cyswllt i'r cyhoeddiad / Link to publication](#)

Dyfyniad o'r fersiwn a gyhoeddwyd / Citation for published version (APA):

Kermanizadeh, A., Powell, L. G., & Stone, V. (2020). A review of hepatic nanotoxicology - summation of recent findings and considerations for the next generation of study designs. *Journal of toxicology and environmental health. Part B, Critical reviews*, 23(4), 137-176. <https://doi.org/10.1080/10937404.2020.1751756>

Hawliau Cyffredinol / General rights

Copyright and moral rights for the publications made accessible in the public portal are retained by the authors and/or other copyright owners and it is a condition of accessing publications that users recognise and abide by the legal requirements associated with these rights.

- Users may download and print one copy of any publication from the public portal for the purpose of private study or research.
- You may not further distribute the material or use it for any profit-making activity or commercial gain
- You may freely distribute the URL identifying the publication in the public portal ?

Take down policy

If you believe that this document breaches copyright please contact us providing details, and we will remove access to the work immediately and investigate your claim.



A review of hepatic nanotoxicology – summation of recent findings and considerations for the next generation of study designs

Ali Kermanizadeh, Leagh G Powell & Vicki Stone

To cite this article: Ali Kermanizadeh, Leagh G Powell & Vicki Stone (2020) A review of hepatic nanotoxicology – summation of recent findings and considerations for the next generation of study designs, Journal of Toxicology and Environmental Health, Part B, 23:4, 137-176, DOI: [10.1080/10937404.2020.1751756](https://doi.org/10.1080/10937404.2020.1751756)

To link to this article: <https://doi.org/10.1080/10937404.2020.1751756>



© 2020 The Author(s). Published with license by Taylor & Francis Group, LLC.



Published online: 23 Apr 2020.



Submit your article to this journal [↗](#)



Article views: 458



View related articles [↗](#)




View Crossmark data [↗](#)

REVIEW



A review of hepatic nanotoxicology – summation of recent findings and considerations for the next generation of study designs

Ali Kermanizadeh ^{a,b}, Leagh G Powell^a, and Vicki Stone^a

^aSchool of Engineering and Physical Sciences, Heriot Watt University, Edinburgh, UK; ^bSchool of Medical Sciences, Bangor University, Bangor, UK

ABSTRACT

The liver is one of the most important multi-functional organs in the human body. Amongst various crucial functions, it is the main detoxification center and predominantly implicated in the clearance of xenobiotics potentially including particulates that reach this organ. It is now well established that a significant quantity of injected, ingested or inhaled nanomaterials (NMs) translocate from primary exposure sites and accumulate in liver. This review aimed to summarize and discuss the progress made in the field of hepatic nanotoxicology, and crucially highlight knowledge gaps that still exist.

Key considerations include

- *In vivo* studies clearly demonstrate that low-solubility NMs predominantly accumulate in the liver macrophages the Kupffer cells (KC), rather than hepatocytes.
- KCs lining the liver sinusoids are the first cell type that comes in contact with NMs *in vivo*. Further, these macrophages govern overall inflammatory responses in a healthy liver. Therefore, interaction with of NM with KCs *in vitro* appears to be very important.
- Many acute *in vivo* studies demonstrated signs of toxicity induced by a variety of NMs. However, acute studies may not be that meaningful due to liver's unique and unparalleled ability to regenerate. In almost all investigations where a recovery period was included, the healthy liver was able to recover from NM challenge. This organ's ability to regenerate cannot be reproduced *in vitro*. However, recommendations and evidence is offered for the design of more physiologically relevant *in vitro* models.
- Models of hepatic disease enhance the NM-induced hepatotoxicity.

The review offers a number of important suggestions for the future of hepatic nanotoxicology study design. This is of great significance as its findings are highly relevant due to the development of more advanced *in vitro*, and *in silico* models aiming to improve physiologically relevant toxicological testing strategies and bridging the gap between *in vitro* and *in vivo* experimentation.

KEYWORDS

Liver; nanomaterials; Kupffer cells; adverse effects; “real” hazard; physiological relevance

Introduction

The rapid expansion and exploitation of engineered nanomaterials (NMs) (“manufactured material in an unbound state or as an aggregate or as an agglomerate and where, for 50% or more of the particles in the number size distribution, one or more external dimensions is in the size

range 1–100 nm” EU commission recommendation 2011) has led to considerable interest in the fields of nanotechnology and nanomedicine (Kermanizadeh et al. 2018; Vance et al. 2015). However, the unique chemical and physical characteristics which make NMs desirable might also contribute to their potential adverse health effects.

CONTACT Ali Kermanizadeh  akz001@yahoo.co.uk  School of Medical Sciences, Bangor University, Bangor, UK

Authors' contributions

© 2020 The Author(s). Published with license by Taylor & Francis Group, LLC.

This is an Open Access article distributed under the terms of the Creative Commons Attribution-NonCommercial-NoDerivatives License (<http://creativecommons.org/licenses/by-nc-nd/4.0/>), which permits non-commercial re-use, distribution, and reproduction in any medium, provided the original work is properly cited, and is not altered, transformed, or built upon in any way.

With the inevitable rise of occupational and general public exposure due to increasing production and utilization of NMs, there is an urgent need to consider the possibility of potential detrimental health consequences of exposure to these materials (Johnston et al. 2012; Kermanizadeh et al. 2015, 2016; Laux et al. 2018). The small size of NMs results in high surface area to volume ratio, which might offer enhanced biological activity per given mass compared to larger-size counterparts (Johnston et al. 2012). Any comprehensive testing strategy for particulates needs to incorporate information on parameters such as surface area, surface chemistry, size distribution and surface charge (Oberdorster et al. 2005). In reality, it is possible that NMs might differ in the severity of toxicity and the mechanism by which adverse effects are exerted.

The lungs and the gastrointestinal tract (GIT) are in continual contact with the external environment and are primary and principal exposure sites for NMs (Laux et al. 2018; Sadauskas et al. 2009). It is well-known that a proportion of NMs translocate to a range of secondary organs with the liver being one of the most important in terms of the quantities of NM accumulation (Balasubramanian et al. 2010; Kermanizadeh et al. 2015; Lee et al. 2013; Lipka et al. 2010). In addition, with constant advances in nanomedicines, these may result in direct entry of NMs into the bloodstream. The presence of NMs in blood might consequently enable in materials reaching the liver rapidly and in large concentrations (Balasubramanian et al. 2010; Kermanizadeh et al. 2015). Therefore, it might be argued that for particulates in the blood, the liver stands in the forefront of a NM challenge.

The liver is the body's main detoxification center, removing waste products (i.e. bilirubin) or foreign substances (Kmiec 2001; Nguyen-Lefebvre and Horuzsko 2015). The organ consists of highly organized parenchyma which is represented by hepatocytes and numerous non-parenchymal cell populations including resident macrophages such as Kupffer cells (KCs) that are involved in xenobiotic elimination (Godoy et al. 2014; Kermanizadeh et al. 2019b, 2014a; Tiegs and Lohse 2010). In particular and of great significance in particle hepatotoxicity is the fact that KCs and sinusoidal endothelial cells line the liver sinusoids.

This organ architecture and environment means that these cells have continuous contact with gut-originated antigens as well as any material, which reaches the organ from the blood. In liver blood flow occurs via the sinusoids which are lined with endothelial cells and KCs. Due to the locality of the KCs in the wall of sinusoids, this sub-population might act as a barrier to the non-soluble NMs, preventing them from reaching the hepatocytes. In addition, activated KCs are one of the most important hepatic cell populations in modulation and governance of the organs immune response both in health and disease states (Bottcher, Knolle, and Stabenow 2011; Kermanizadeh et al. 2014a; Tiegs and Lohse 2010; Zhu et al. 2017).

This review is a follow-up to our 2013 review published in British Journal of Pharmacology (Kermanizadeh et al. 2014b). The aim of this investigation was to highlight the progress made in the research in the area of NM-induced hepatic toxicity since 2013 and the knowledge gaps that still exist. The main body of the manuscript summarizes a wide range of relevant studies carried out between 2013 and 2019, which focused on hepatic NM-induced adverse effects, bio-accumulation *in vivo*, or toxicity using *in vitro* or *ex vivo* models. Each study was intentionally segregated and abridged in detail to enable the reader real context and providing important and relevant experimental detail. The search criteria included a combination of the following terms: "nanoparticles," "nanomaterials," "hepatic," "liver," "liver tissue," "toxicity," "cytotoxicity," "adverse effects," "bio-distribution," "distribution," "translocation," "hepatocytes," "HepG2" "HepaRG," "C3A," "Chang cells," "gastrointestinal tract," "Kupffer cells," "primary liver cells," "primary hepatic cells," "oral exposure," "intravenous exposure," "dermal exposure" and "inhalation." The last literature search was conducted on 16-12-2019.

Due to the inevitable limitations and exclusionary nature of any literature search; studies that did not include the search terms in the title or did not provide adequate information in the abstract might have been unintentionally omitted. However, importantly all relevant negative data from the investigations in which hepatic toxicity or bioaccumulation was investigated but not

observed are included (and highlighted in Table 1). The focus of the review is primarily based upon human and rodent models as these have been the predominant investigated experimental models in the literature, although a few studies in other models do such as aquatic, invertebrate or avian species exist (Al-Badri et al. 2019; Campbell et al. 2018; Gao et al. 2018; Gagne et al. 2013; Hernandez-Moreno et al. 2019; Lekamge et al. 2019; Lecave et al. 2018; Ramachandran et al. 2018). Further, any study that did not provide adequate material characterization data were excluded. This review only focused on engineered NMs and not nanomedicines (nanocarriers or solid drug NMs) or naturally occurring compounds. Finally, from a toxicological perspective, it is important to state that investigations which utilized high non-physiological concentrations/doses are included in this review as these are a prominent and representative proportion of the current NM-induced liver toxicology research landscape. This issue will be highlighted on an individual basis. The main body of text only includes a selection of representative publications over the last 5 years. However, Table 1 contains all studies that were identified as suitable for this literature review, with the overall conclusions and recommendations based upon all the literature summarized in Table 1.

The review is structured into *in vivo* (further segregated by route of exposure and solubility of the NM being discussed) and *in vitro/ex vivo* sections. The final section concludes with a summation of the progress made in the field since 2013, along with our thoughts on the areas of research, which are still lacking and some recommendations for future and progression of hepatic nanotoxicology.

Engineered NMs and the liver – *in vivo* studies

Intravenous (iv) route of exposure

Intravenous (iv) exposure of male Sprague-Dawley rats weighing approximately 150 g to a 20 nm Ag NM at a single dose of 50 mg/kg for 24 hr resulted in significantly increased activities of serum aspartate transaminase (AST) by 54%, alanine

transaminase (ALT) by 76%, acid phosphatase (ACP) by 82% and alkaline phosphatase (ALP) by 85%, compared to control rats (Kumar and Abraham 2016). Further, the Ag NM-treated rats exhibited decreased activities of catalase and superoxide dismutase (SOD) and higher concentrations of thiobarbituric acid reactive substances (TBARS) compared to controls. These serum biomarkers are traditionally utilized as indicators of liver damage. Finally, Ag treatment resulted in eosinophilic necrosis of hepatocytes, dilated central vein and focal inflammatory cell infiltration in the examined liver sections (Kumar and Abraham 2016).

In another study, the role of KC in the immunotoxicological hepatic response to Ag NMs (approximately 50 nm) was investigated in 10-week-old female C57BL/6 mice following a single IV exposure (Kermanizadeh et al. 2014a). In these experiments, the KC population was reduced via iv administration of clodronate liposomes for 48 hr prior to animals receiving NMs (24 µg per animal) for periods of 24, 48 or 72 hr. In the livers in which the KC population was specifically destroyed the levels of inflammatory cytokines were significantly decreased compared to controls. Kermanizadeh et al. (2014a) also noted high levels of interleukin (IL) 10 released from Ag treated hepatic tissue of normal mice in comparison to KC depleted livers, suggesting involvement of the KCs in orchestrating an anti-inflammatory response to a low dose NM challenge in a healthy liver. It is noteworthy that IL10 is a potent anti-inflammatory cytokine involved in the maintenance of immune tolerance in a healthy organ.

The adverse hepatic effects of iv administration of Ag NM (approximately 30 nm) were investigated in models of alcoholic hepatic disease *in vitro* and *in vivo*. In this set of trials, 8-week-old female C57BL/6 mice were divided into two groups with one receiving an all liquid diet for 25 days while the other group were fed an all liquid diet supplemented with 5% ethanol. The animals were injected with a single dose of either 25 or 100 µg of the NMs for 24 or 168 hr. Kermanizadeh et al. (2017a) demonstrated that NM-induced adverse hepatic health effects were significantly enhanced in alcohol-fed mice in

Table 1. The summary of the accumulation and adverse effects of nanomaterials on the liver from studies 2013–2019 following exposure via IV, oral, inhalation, IT, intranasal, IP and dermal routes.

| NM | Size | Route of NM exposure | Species | Dose | Number of exposures | Exposure duration | Hepatic effects | Histopathology | Recovery period included/ Hepatic recovery observed | Reference |
|--|--------|----------------------|--------------------------------------|---------------------|---------------------|-------------------|---|---|--|---------------------------|
| Ag | 20 nm | IV | Sprague-Dawley rats | 50 mg/kg | 1 | 24 hr | Increased AST, ALT, ACP, ALP, TBARS and decreased CAT, SOD | Necrosis of hepatocytes, dilated central vein and focal inflammatory cell infiltration | No | Kumar and Abraham 2016 |
| PVP-coated Ag | 5 nm | IV | B6C3F1 mice | 25 mg/kg | 1 or 3 | 24 hr | All NMs induced oxidative DNA damage | Not analyzed | No | Li et al. 2014 |
| PVP-coated Ag | 50 nm | | | | | | | | | |
| silicon-coated Ag | 45 nm | | | | | | | | | |
| Citrate or PVP coated Ag | 10 nm | IV | CD-1 mice | 10 mg/kg | 1 | 24 hr | Not analyzed | Lesions in the liver present and NM size-dependent | No | Recordati et al. 2015 |
| | 40 nm | | | | | | | | | |
| | 100 nm | | | | | | | | | |
| Ag | 50 nm | IV | C57BL/6 mice | 24 µg/animal | 1 | 24, 48 or 72 hr | KC mediated anti-inflammatory response | Not analyzed | No | Kermanizadeh et al. 2014a |
| Ag | 30 nm | IV | Healthy and alcohol fed C57BL/6 mice | 25 or 100 µg/animal | 1 | 24 or 168 hr | Inflammatory response, changes in blood biochemistry, acute phase response (all aggravated in the diseased animals) | Changes in intrahepatic architecture, granuloma formation, hepatocyte necrosis, parenchymatous degeneration and the destruction of the liver plates | Yes/Yes | Kermanizadeh et al. 2017a |
| Au | 10 nm | IV | Sprague-Dawley rats | 10 or 100 µg/kg/day | 1 | Up to 4 weeks | NM accumulation only/no adverse effects | Not analyzed | No | Lee et al. 2018 |
| Ag or mix | 10 nm | | | | | | | | | |
| Superparamagnetic zinc-cobalt ferrite | 8 nm | IV | New Zealand rabbits | 20 mg/animal | 1 | 4 hr | Not analyzed | Granuloma formation and multiple congestions | No | Hanini et al. 2016 |
| ZnO QD | 5 nm | IV | Kunming mice | 5 mg/kg | 7 daily doses | 1–7 days | No changes in ALT and AST activity | Not analyzed | No | Yang et al. 2014 |
| PEGylated-ZnO QD | 95 nm | | | | | | | | | |
| Zn-labeled CdSe/CdS/ZnS-QD | 11 nm | IV | FVB/N mice | 50–100 pmol/animal | 1 | 2 hr | Not analyzed | Accumulation in KCs but not hepatocytes | No | Bargheer et al. 2015 |
| MEA and MPA coated Ag ₂ Se QD | 5 nm | IV | CD-1 mice | 8 µmol/kg | 1 | 2 min – 28 days | Not analyzed | Mild edema in the liver in the QDs-MEA group | Yes/No | Tang et al. 2017 |
| Oleic acid PEGylated CdSeS/ZnS QD | 60 nm | IV | Wistar rats | 14 µg/animal | 1 | 12 hr | QDs predominately taken up by KCs | Not analyzed | No | Tsoi et al. 2016 |

(Continued)

Table 1. (Continued).

| NM | Size | Route of NM exposure | Species | Dose | Number of exposures | Exposure duration | Hepatic effects | Histopathology | Recovery period included/ Hepatic recovery observed | Reference |
|--|--|----------------------|--|-----------------------------|-------------------------|-------------------|--|---|--|-----------------------|
| CdTe-QD | ~ 15 nm | IV | BALB/c mice | 0.4, 2, 5, 6, 7 or 10 mg/kg | 1 | 24 hr | Increases in AST, ALT, total bilirubin and SAA levels, reduced albumin levels at the highest doses | 6 mg/kg bw and higher induced liver hemorrhage observed in the periportal areas of the hepatic lobules accompanied by apoptotic and necrotic liver cells in those areas | No | Nguyen et al. 2019 |
| Carboxyl coated CdSe/ZnS QD | 20 nm | IV | Pregnant and offspring Sprague-Dawley rats | 1 or 5 nmol | 1 | Up to 180 days | Increased ALT, AST, bilirubin and gamma glutamyl transaminase in the mothers | Hepatic cellular apoptosis, necrosis, cytolysis, loss of hepatic lobules in the livers of exposed animals at day 1 post exposure | Yes/Yes | Yang et al. 2018a |
| SiO ₂ | ~ 150 nm | IV | Sprague-Dawley rats | 50 mg/kg | 1 | 48 hr | Increased AST, total bile acid, cholesterol, and low-density lipoprotein levels | Increase in the number of the KCs | No | Chen et al. 2017 |
| SiO ₂ | 50 nm | IV | Athymic nude mice | 20 mg/kg | 1 | Up to 7 days | Increase in ALT and catalase activity | Not analyzed | Yes/Yes | Baati et al. 2016 |
| SiO ₂ Fe-SiO ₂ hollow nano shells | 500 nm 500 nm | IV | Swiss white mice | 2–20 mg/kg | 1 | 24 hr | No changes in serum biochemistry | Only mild pathology manifested as lymphocytic infiltration | Yes/Yes | Mendez et al. 2017 |
| SiO ₂ | 110 nm | IV | WT BALB/c or NLRP3 ^{-/-} or Caspase 1 ^{-/-} mice | 25 or 50 mg/kg | 3 doses every other day | 3 weeks | Increased serum ALT and AST, inflammatory response | Not analyzed | Yes/Yes | Zhang et al. 2018 |
| Hexagonal copper sulfide nanoplate | Length of 59 nm and thickness of 24 nm | IV | ICR mic | 7.7 to 550 mg/kg | 1 | 48 hr | Not analyzed | No pathology | No | Feng et al. 2015 |
| Polyacrylic acid-coated iron oxide | ~ 10 nm | IV | CD-1 mice | 8, 20 or 50 mg/kg | 1 | 24 hr | Not analyzed | Necrotic hepatocytes, NM only visible in KCs | No | Rodrigues et al. 2017 |

(Continued)

Table 1. (Continued).

| NM | Size | Route of NM exposure | Species | Dose | Number of exposures | Exposure duration | Hepatic effects | Histopathology | Recovery period included/ Hepatic recovery observed | Reference |
|--|--|----------------------|------------------------------------|-----------------------------|---------------------|---------------------|--|---|--|-----------------------------|
| Iron oxide magnetic NMs coated with PEG, BSA and COOH | all ~ 50 nm | IV | Sprague-Dawley rat | 50 mg/kg | 2 | Up to 24 days | Day 1 postinjection ALT, AST, total protein increased by PEG and COOH NMs; ALT, AST, total protein increased by BSA and COOH NMs | No significant histological alternations were detected | Yes/Yes | Yang et al. 2018b |
| Au/FeO ₄ NMs coated with amphiphilic polymer or PEG | ~ 100 nm | IV | C57/BL6 mice | 56 µg iron | 1 | Up to 365 days | NMs detectable in KCs for up to 1 year | No pathology | Yes/NA | Kolosnjaj-Tabi et al. 2015 |
| Au nanorod | 220 nm | IV | CD-1 mice | 5 mg/kg | 1 | Up to 28 days | Increased γ-glutamyltransferase, bilirubin and total bile decreased SOD, GSH and GSH-Px | No histological alternations were detected – exclusively in the KCs | Yes/Yes | Cai et al. 2016 |
| Au | ~ 15 nm | IV | BALB/c mice F344 rats | 1000 mg/kg | 1 | Up to 28 days | No changes in serum biochemistry | Micro-granulomas, NMs predominately in KC | Yes/Yes | Bahamonde et al. 2018 |
| Au prisms | 10 nm with three edge lengths of ~150 nm | IV | Swiss mice | 6 µg/g | 1 | 72 hr or 4 months | No serum biochemistry alterations | Enlarged vacuoles, NM accumulation in KCs | Yes/NA | Pérez-Hernández et al. 2017 |
| Au | 10 nm 50 nm rods 60 × 30 nm stars 55 nm | IV | CD-1 mice | 1.54 × 10 ¹⁰ NMs | 1 | Up to 120 hr | Not analyzed | No pathology | No | Talamini et al. 2017 |
| Chitosan-capped star Au | ~ 110 nm | IV | BALB/c mice | 2 mg/kg | 1 | 2 mg/kg | Toxicity not analyzed/NM accumulation in the liver | Not analyzed | No | Wang et al. 2015 |
| Au nanorod | 18 nm width, 58 nm length | IV | Kunming mice | 3 mg/kg | 1 | Up to 90 days | No serum biochemistry alterations | Not analyzed | Yes/NA | Li et al. 2018b |
| PEGylated Au | ~ 6 nm 25 nm 40 nm 60 nm | IV | | | | | | | | |
| Dextran coated Au | 20 nm | IV | Athymic nude mice | 1 mg/kg | 1 | 24 hr, 7 or 14 days | No serum biochemistry alterations | No pathology | Yes/NA | Bailey et al. 2019 |
| TiO ₂ | ~ 150 nm | IV | C57BL/6 J gpt mice | 2, 10 and 50 mg/kg | 4 (once a week) | 4 weeks | No genotoxic effect observed | NM accumulation in KCs | No | Suzuki et al. 2016 |
| TiO ₂ | ~ 20 nm | IV | C57BL/6 mice (with PUR288 plasmid) | 10 or 15 mg/kg/day | 2 | 28 days | No genotoxic effect observed | Not analyzed | Yes/NA | Louro et al. 2014 |

(Continued)

Table 1. (Continued).

| NM | Size | Route of NM exposure | Species | Dose | Number of exposures | Exposure duration | Hepatic effects | Histopathology | Recovery period included/ Hepatic recovery observed | Reference |
|---|---|----------------------|----------------------------------|---------------------------------|---------------------|-------------------|--|---|--|----------------------|
| Ni | ~ 50 nm | IV | Sprague Dawley rats | 1, 10 or 20 mg/kg | 1 | 14 days | Increase in biomarkers of liver damage | Mild damage – distorted architecture of the sinusoids | Yes/No | Magaye et al. 2014 |
| PEGylated platinum | 2–4 nm | IV | BALB/c mice | 5, 10, 15 and 20 mg/kg | 1 | 24 hr | No serum biochemistry alterations | No pathology | No | Brown et al. 2018 |
| Alumina nanotube | ~ 700 nm long and 90 nm in diameter) | IV | BALB/c mice | 20, 50, 100 mg/kg | 1 | Up to 28 days | Infiltration of inflammatory cells in the livers | No pathology | Yes/Yes | Wang et al. 2017 |
| AlO | 90 nm | IV | ICR mice | 1.5 or 5 mg/kg | 1 | Up to 14 days | No changes in serum biochemistry | Inflammatory cell infiltration | Yes/NA | Park et al. 2016a |
| ZrO ₂ | 150 nm | IV | ICR mice | 300, 400, 500 and 600 mg/kg | 1 | 14 days | Increased serum ALT levels at 500 mg/kg | No pathology | No | Yang et al. 2019 |
| Reduced graphene oxide | ~ 350 nm | IV | Wistar rats | 7 mg/kg | 1 | 1, 3 hr or 7 days | No serum biochemistry alterations were detected | No pathology | No | Mendonça et al. 2016 |
| Graphene oxide functionalized with poly sodium Up to 16 mg/kg | 1 | Up 180 days | Increase in ALT and AST activity | Black lesions mostly in the KCs | Yes/Yes | Wen et al. 2015 | 4-styrenesulfonate | ~ 700 nm | IV | BALB/c mice |
| Nanoclay | Mixed material size of ~ 60 or ~ 650 nm | IV | BALB/c male mice | Up to 20 mg/kg | 1 | 24 hr | Increased ALT and AST activity | Large regions of cellular necrosis | No | Isoda et al. 2017 |
| Mesoporous Si coated bioactive glass NMs | ~ 250 nm | IV | ICR mice | 20, 100 and 180 mg/kg/day | 14 | 14 days | Increased ALP at the highest dose | Lymphocytic infiltration and granuloma formation | No | Mao et al. 2016 |
| SiO ₂ | 200 nm | IV | C57BL/6 mice | 100 mg/kg | 1 | 24 hr | Increased LC3-II in hepatocytes | Not analyzed | No | Zhang et al. 2017 |
| Lanthanide-based upconversion NM | ~ 40 nm | IV | WT and KC depleted C57BL/6 mice | 150 mg/kg | 1 | 24 hr | Increased ALT and most evident in KC depleted mice | Infiltration of inflammatory cells and most evident in KC depleted mice | No | Zhu et al. 2017 |
| Ag stabilized by PVP or citrate stabilized | 20 nm 110 nm | Oral | C57BL/6 mice | 0.1, 1 or 10 mg/kg/day | 3 | Up to 9 days | Not analyzed | No pathology | No | Bergin et al. 2016 |

(Continued)

Table 1. (Continued).

| NM | Size | Route of NM exposure | Species | Dose | Number of exposures | Exposure duration | Hepatic effects | Histopathology | Recovery period included/ Hepatic recovery observed | Reference |
|---|---|----------------------|------------------------------|-----------------------|---------------------|-------------------|---|---|---|--------------------------------------|
| Ag | ~ 10 nm | Oral | Sprague-Dawley rats | Up to 100 mg/kg/day | 5 | 5 days | Increased ROS, DNA damage, ALT, AST and ALP at highest doses) | Hepatocytes disruption, hepatocellular vacuolation, and central vein injury | No | Patolla, Hackett, and Tchounwou 2015 |
| Citrate-modified Ag | 20 nm | Oral | Wistar rats | 40 mg/kg | 1 | 4 weeks | Changes in proteins expression associated with oxidative stress, inflammatory response, oxidation and deamination | Lymphocyte infiltration and swelling of hepatocytes | Yes/NA | Xie et al. 2018 |
| Ag | ~ 10 nm | Oral | Pregnant Sprague-Dawley rats | Up to 1000 mg/kg | 13 | 13 days | Decrease in catalase and GSH in maternal livers at the higher doses | Not analyzed | No | Yu et al. 2014 |
| Ag MWCNT | ~ 10 nm Diameter 20–30 nm and length | Oral | Swiss albino mice | 50 or 100 mg/kg | 14 | 28 days | Dose dependant DNA damage for both NMs | Not analyzed | No | Awasthi et al. 2015 |
| ZnO | 5–50 μ m ~ 30 nm | Oral | Sprague-Dawley rats | 125, 250 or 500 mg/kg | 90 | 90 days | Decrease in total serum protein and albumin at the highest dose | No pathology | Yes/NA | Park et al. 2014 |
| Silica shell with either fluorescent Rhodamine 6 G core or CdSe/CdS/ZnS QDs as the core | ~ 30 nm | Oral | Mice (species not specified) | 0.1 or 0.67 mg/animal | 4 | 4 days | NM accumulation in the liver | Not analyzed | No | Zane et al. 2015 |
| ZnO | 50 nm | Oral | ICR mice | Up to 10,000 mg/kg | 14 | 14 days | Increased serum AST and ALT activity | Infiltration of inflammatory cells in the portal regions of liver | No | Kong et al. 2018 |
| ZnO | 20 and ~ 200 nm | Oral | ICR mice- model of IBD | 1 g/kg | 1 | 24 hr | Higher quantities of ZnO detected in the diseased animals | Not analyzed | No | Du et al. 2018 |

(Continued)

Table 1. (Continued).

| NM | Size | Route of NM exposure | Species | Dose | Number of exposures | Exposure duration | Hepatic effects | Histopathology | Recovery period included/ Hepatic recovery observed | Reference |
|--|----------------|----------------------|--|--|---------------------|-------------------|--|--|--|-------------------------|
| ZnO NMs and elemental Pb | ~ 14 and 60 nm | Oral | C57BL/6 mice normal or high fat diets | NMs only – 200 mg/kg or NMs/Pb – 200 and 150 mg/kg daily | 14 | 14 days | Reduction in SOD and increase in MDA | Spotty cell necrosis and a mild vacuolar degeneration | No | Jia et al. 2017 |
| ZnO nanorod | ~ 20 nm | Oral | Swiss albino mice | Up to 6 mg/kg | 7 | 7 days | Not analyzed | No pathology | No | Bollu et al. 2016 |
| ZnO | 80–100 nm | Oral | Swiss albino mice | 500 mg/kg/day | 21 | 21 days | Increased ROS and decreased SOD and catalase activity | No histological alternations were detected, TiO ₂ detectable only in KCs | No | Shrivastava et al. 2014 |
| TiO ₂ | 50–75 nm | | | | | | | | | |
| Al ₂ O ₃ | 40–50 nm | | | | | | | | | |
| SiO ₂ | ~ 15 nm | Oral | Kun-Ming mice – healthy or metabolic syndrome model | 10 mg/kg/day | 30 | 30 days | Increased hepatic DNA damage in the metabolic syndrome mice post NM administration | Increased hepatocyte ballooning and infiltration of inflammatory cells, collagen deposition in metabolic syndrome mice post NMs administration | No | Li et al. 2018a |
| SiO ₂ | ~ 20 nm | Oral | C57BL/6 transgenic mouse model, expressing the human mutated (A53 T) α-synuclein protein (TgHuA53 T) | NMs in drinking water for up to 18 months | - | Up to 18 months | Not analyzed | Minor inflammatory cell infiltration in the portal and lobular regions | No | Boudard et al. 2019 |
| SiO ₂ | ~ 35 nm | Oral | Sprague-Dawley rats | 1000 mg/kg | 91 | 13 weeks | Ag NM induced slight increase in serum ALP | Not analyzed | No | Yun et al. 2015 |
| Ag | ~ 20 nm | | | | | | | | | |
| Fe ₃ O ₃ | ~ 120 nm | | | | | | | | | |
| Zn ²⁺ -doped Fe ₃ O ₄ | ~ 10 nm | Oral | Mice (species unspecified) | 50 mg/kg/day | 30 | 30 days | Increased LDH, ALT, AST, TBIL and GSH-Px | No pathology | No | Zhu et al. 2016 |
| Cu NM | ~ 30 nm | Oral | Sprague-Dawley rats | 100, 200 and 400 mg/kg/day | 28 | 28 day | NM-induced increased AST, ALT and total bilirubin activity but not microparticles | Not analyzed | No | Lee et al. 2016 |
| Cu microparticle | ~ 25 μm | | | | | | | | | |

(Continued)

Table 1. (Continued).

| NM | Size | Route of NM exposure | Species | Dose | Number of exposures | Exposure duration | Hepatic effects | Histopathology | Recovery period included/ Hepatic recovery observed | Reference |
|-----------------------------------|--|----------------------|--|--------------------------------|---------------------|----------------------------|---|--|--|-------------------------|
| Tin sulfide nanoflowers | 50, 80 and 200 nm | Oral | ICR mice | 250–1000 mg/kg | 14 | 14 day | Increased serum ALT and AST and altered liver metabolic genes – 50 nm NMs at the highest dose | Slightly disrupted cellular arrangement, moderate interstitial hyperemia, sporadic and focal infiltration of inflammatory cells at the highest dose | No | Bai et al. 2018 |
| CdS nanorod and cubic CdS nanodot | 30–50 nm diameter, 500–1100 nm length ~ 5 nm | Oral | Kunming mice | Up to 200 mg/kg | 18 or 35 | 18 or 35 days | Not analyzed | Infiltration of inflammatory cells and hepatocellular vacuolation, higher for nanodots | No | Liu et al. 2014 |
| Au | ~ 8 nm | Oral | Healthy and alcohol and methamphetamine injury Wistar rats | 181.48, 362.48 or 724.96 µg/kg | 3 | 28 days | NM induced protective effects against alcohol and methamphetamine disease | No pathology | No | de Carvalho et al. 2018 |
| TiO ₂ | ~ 300 nm | Oral | Swiss albino mice | 10, 50 or 100 mg/kg/day | 14 | 14 days | Increased AST and decreased GSH levels, Increased DNA damage, p53, BAX, caspase 3 and 9 | Not analyzed | No | Shukla et al. 2014 |
| TiO ₂ | ~ 75 nm | Oral | Young and old Sprague-Dawley rats – aging model | 200 mg/kg/day | 30 | 30 days | Small changes in serum biochemistry relating to liver damage | Edema, hepatic cord disarray, cell swelling, vacuolization and hydropic degeneration in young but not old rats | No | Wang et al. 2013 |
| TiO ₂ | ~ 100 nm | Oral | Wistar rats | 0.5, 5, and 50 mg/kg/day | 14 | 14 days | No change in GSH levels, significant decrease in TBARS levels | Not analyzed | No | Canli et al. 2020 |
| TiO ₂ | ~ 100 nm | Oral | Wistar rats | 0.5, 1; 4; and 16 g/kg | 1 | 4 days, 30 days or 60 days | Not analyzed | Necrosis in the hepatocytes located around the centrilobular veins only, TiO ₂ aggregates visible inside Kupffer cells located in the sinusoids | Yes/NA | Valentini et al. 2019 |

(Continued)

Table 1. (Continued).

| NM | Size | Route of NM exposure | Species | Dose | Number of exposures | Exposure duration | Hepatic effects | Histopathology | Recovery period included/ Hepatic recovery observed | Reference |
|--|--|----------------------|---------------------|---|---------------------|-------------------|---|---|--|-----------------------------|
| TiO ₂ | 29 nm | Oral | Sprague Dawley rats | 2, 10 and 50 mg/kg daily | 90 | 90 days | Increased levels of total protein, albumin and globulin, decreased levels of total bilirubin, ALT, AST, decreased GSH, lipid peroxidation and increased GSH-Px and SOD activity | Fatty degeneration of hepatocytes | No | Chen et al. 2019 |
| Cr ₂ O ₃ | ~ 24 nm | Oral | Wistar rats | 100 or 200 µg/g | 1, 7 or 14 | 1, 7 or 14 days | Dose dependant increase in AST, ALT, ALP, γGT, and total bilirubin levels | 7 day exposures resulted in severe hemorrhage, hepatocyte degeneration, and parenchymal distortions | No | Fatima and Ahmad 2019 |
| Fullerene C ₆₀ | | Oral | Sprague-Dawley rats | 1 day –2000 mg/kg 30 days- 250 mg/kg/day | 1 or 30 | 24 hr or 30 days | No hematological or serum biochemistry alterations were detected | Not analyzed | No | Hendrickson et al. 2015 |
| Graphene oxide | | Oral | Swiss albino mice | 10, 20 or 40 mg/kg daily | 1 or 5 | 1 or 5 | Not analyzed | Apoptosis, necrosis and cells degeneration | No | Mohamed et al. 2019 |
| γ-aluminum oxide hydroxide γ- and α-aluminum oxide NMs Al ₂ Si ₂ O ₅ (OH) ₄ nanotube | All 180–200 nm ~ 400 nm | Oral | ICR mice | 5 or 10 mg/kg | 1 | 24 hr | Accumulation in the liver | Not analyzed | No | Park et al. 2016b |
| | | Oral | Kunming mice | 5–300 mg/kg | 30 | 30 days | Decreased GSH-Px and SOD activity | At the highest dose – hydropic degeneration with swelling of hepatocytes | No | Wang et al. 2018b |
| Co-exposure Ag and TiO ₂ | Ag – ~ 90 nm TiO ₂ – ~ 50 nm | Oral | Wistar rats | 0.5 mg/kg daily dose | 45 | 45 days | Decreased GSH-Px, no genotoxicity | Not analyzed | No | ADC et al. 2017 |
| Ag | ~ 20 nm | IT | C57/BL6 mice | Up to 128 µg/animal | 1 | 24 hr | Dose dependant decrease in GSH levels | Not analyzed | No | Gosens et al. 2015 |
| Non-functionalized and coated ZnO | 100 nm | | | | | | | | | |
| Zn | ~ 40 nm | Inhalation | C57BL/6 mice | 4 hr/day~3.5 mg/m ³ | 14 or 91 | 2 or 13 weeks | No hepatic toxicity or accumulation | No pathology | Yes/NA | Adamcakova-Dodd et al. 2014 |

(Continued)

Table 1. (Continued).

| NM | Size | Route of NM exposure | Species | Dose | Number of exposures | Exposure duration | Hepatic effects | Histopathology | Recovery period included/ Hepatic recovery observed | Reference |
|---|---|--------------------------|---------------------|---|---------------------|--|---|---|---|-----------------------|
| Pristine TiO ₂ | ~ 400 nm | Oropharyngeal aspiration | BALB/c mice | 20 µg/animal/ week | 5 | 5 weeks | Accumulation of Ag and SiO ₂ in the liver | Not analyzed | Yes/NA | Smulders et al. 2014 |
| Pristine Ag | ~ 90 nm | | | | | | | | | |
| Pristine SiO ₂ | ~ 190 nm | | | | | | | | | |
| Aged paints containing NMs | | | | | | | | | | |
| ZnO | ~ 30 nm | Nose only | Sprague-Dawley rats | 2.56 mg per exposure | 1 or 7 | Up to 7 days | Significant increases in serum (IL-1α, IL-1β, IL-10 and TNFα) Elevated SOD and CAT, MDA and ROS in liver | Not analyzed | No | Guo et al. 2020a |
| CuO | ~ 10 nm | Nose-only | Wistar rat | 0.6–13.2 mg/m ³ | 5 | 5 days | No NM accumulation or adverse effects in the liver | No pathology | No | Gosens et al. 2016 |
| CeO ₂ | ~ 35 nm | Nose only | ICR mice | 40 mg/kg per day | 3 | 7 days | Decreased serum levels of total bilirubin and ALP | Hydropic degeneration | No | Liu et al. 2019 |
| 4 different NIO NMs Fully characterized | ~ 300 nm | IT | F344 rats | Up to 6 mg/kg | 1 | 91 days | No NM accumulation or adverse effects in the liver | Not analyzed | Yes/NA | Shinohara et al. 2017 |
| NiO | ~ 80 nm | IT | Wistar rats | 0.015–0.24 mg/kg | 12 | 6 weeks | Small decreases in catalase, GSH Px and SOD activity | Highest NM dose – neutrophil and lymphocyte infiltration and sporadic spotty necrosis | No | Yu et al. 2018 |
| TiO ₂ | ~ 25 nm | IT | Sprague-Dawley rats | 0.5, 2.5 and 10 mg/kg | 3 | 3 or 35 days | Increased DNA damage – not dose dependant | Not analyzed | Yes/NA | Reller et al. 2017 |
| TiO ₂ | -ve ~ 50 nm +ve ~ 1500 nm | IT | C57BL/6 mice | 18, 54 or 162 µg/animal | 1 | 24 hr | Increased DNA damage and saa3 mRNA levels | Not analyzed | No | Wallin et al. 2017 |
| TiO ₂ | 10 nm | IT | C57BL/6 mice | Up to 128 µg/animal | 1 | 24 hr | Increased GSH levels | Not analyzed | No | Vranic et al. 2017 |
| Graphite nanoplates | 20 µm lateral, 5 µm lateral <2 µm lateral and 8–25 nm | Pharyngeal aspiration | C57BL/6 mice | 4 or 40 µg | 1 | 4 hr, 1 day, 7 days, 1 month or 2 months | Increased acute phase genes at higher dose at 4 hr and 1 day post exposure | Not analyzed | Yes/Yes | Roberts et al. 2015 |
| CNT | | | | | | | | | | |
| Sanding dust from an epoxy composite with (0.2%) or without CNT | Diameter ~ 15 nm; length 4 µm | IT | C57BL/6 mice | NM – 18, 54 and 162 µg/animal Dust – 54, 162 and 486 µg/animal | 1 | Up to 28 day | Increased <i>Saa1</i> expression | CNT and epoxy dust with CNTs – inflammatory cell infiltrations | Yes/Yes | Saber et al. 2015 |

(Continued)



Table 1. (Continued).

| NM | Size | Route of NM exposure | Species | Dose | Number of exposures | Exposure duration | Hepatic effects | Histopathology | Recovery period included/ Hepatic recovery observed | Reference |
|--|-------------------------------------|----------------------|-------------------------------|---|---|-------------------|---|--|--|-------------------------------|
| ZnO | 10–30 nm | IP | Wistar rats | 50–200 mg/kg/day | 10 | 10 days | Increased ALT at the highest doses | Increased numbers of KCs, inflammation in the liver parenchyma, hepatocyte ballooning and chromatin condensation. | No | Abbasalipourkabir et al. 2015 |
| ZnO | ~ 35 nm | IP | Wistar albino rats | 2 mg/kg/day | 21 | 21 days | Not analyzed | Sinusoidal dilatation, KC hyperplasia, inflammatory cells infiltration, necrosis, hydropic degeneration, apoptosis | No | Almansour et al. 2017 |
| Ag ₃ Cu ₂ B sphere | ~ 100 nm | IP | C57BL/6 NLRP3 KO BALB/c mice | 1–20 mg/kg | 1 | 24 or 96 hr | WT had increased AST, ALT and LDH, KO mice had diminished immune response | Hepatic necrosis, increased sinusoidal KCs, granuloma formation | No | Ramadi et al. 2016 |
| Fe ₃ O ₄ | ~ 35 nm | IP | Kun Ming mice | NM – 30 mg/kg/day and elemental CdCl ₂ – 1 mg/kg/day | 7 | 7 days | No serum biochemistry alterations | Swelling in hepatocytes around the central vein NM reduced CdCl damage. | No | Zhang et al. 2016 |
| TiO ₂ nanosheets | 92.5 nm | IP | C57BL/6 mice | 10 mg/kg | 1 | Up to 30 days | NM accumulation in the liver | No pathology | Yes/NA | Song et al. 2014 |
| TiO ₂ | ~ 50 nm | IP | Swiss Webster mice | 500, 1000 or 2000 mg/kg/day | 5 | 5 days | Co-administration of anti-oxidant and TiO ₂ decreased NM-induced increases in MDA, GSH, SOD, catalase, GSH Px and DNA damage | Not analyzed | No | El-Ghor et al. 2014 |
| MWCNT mesoporous SiO ₂ NMs | 110–170 nm and 5–9 nm length ~ 8 nm | IP | Swiss albino mice | MWCNT – 1.5, 2 and 2.5 mg/kg SiO ₂ – 10, 25 and 50 mg/kg | 1 | 7 days | Increase in AST activity for MWCNT not SiO ₂ | Not analyzed | Yes/NA | Rawat et al. 2017 |
| Dextran coated ferrite NM | ~ 85 nm | Dermal | Guinea pig | 80 mg/animal/3 times a week | 9 | 3 weeks | No serum biochemistry alterations | Not analyzed | No | Mohanan et al. 2014 |
| Tattoo ink | NA | Dermal | C3.Cg/TifBomTac hairless mice | NA | 1 | 365 days | Ink pigment deposits in KCs one year after exposure | Not analyzed | Yes/NA | Sepehri et al. 2017 |
| MULTIPLE ROUTES OF EXPOSURE | | | | | | | | | | |
| Ag | 10 nm 50 nm 100 nm | IV Oral | Lactating BALB/c mice | 1.5 mg/kg 1.5 mg/kg | 4 x 4 hr exposed 4 hr exposed ₁ | 21 days | No adverse effects reported | Not analyzed | No | Morishita et al. 2016 |

(Continued)

Table 1. (Continued).

| NM | Size | Route of exposure | Species | Dose | Number of exposures | Exposure duration | Hepatic effects | Histopathology | Recovery period included/ Hepatic recovery observed | Reference |
|----------------------------------|--------------------------|---|---------------------|--|---------------------|-------------------|---|--|---|------------------------|
| ZnO | ~ 35 nm | IV Oral | Sprague-Dawley rats | 3 mg/kg 30 mg/kg | 1 | Up to 7 days | Significant elevation in levels of AST in IV exposed animals No changes in serum biochemical parameters were observed in orally administered | No Pathology | No | Choi et al. 2015 |
| Cu ZnO | 16–96 nm 16–96 nm | IP IV | Wistar rats | Cu –6.1–19.82 µg/kg ZnO – 11.14–30.3 µg/kg | 1 | 14 or 28 days | Increased serum creatinine, ALT, ALP and AST levels (more significant for the IP route) | Not analyzed | Yes/NA | Ashajyothi et al. 2018 |
| SiO ₂ | 110 nm | IV Hypodermic Intramuscular Oral | ICR mice | 50 mg/kg | 1 | 24 hr or 7 days | NM accumulation in the liver – highest quantities following IV exposure | No pathology | Yes/NA | Fu et al. 2013 |
| SiO ₂ | ~ 20 nm | IT IV | Sprague-Dawley rats | 9, 18 or 36 mg/kg 15, 30 or 60 mg/kg | 1 | Up to 48 hr | No DNA damage | Not analyzed | No | Guichard et al. 2015 |
| 5 different TiO ₂ NMs | NMs fully characterized | Oral | Wistar rats | 2.3 mg/rats | 1 or 5 | 24 hr or 5 days | NM accumulation and bio-persistence in the liver | Not analyzed | Yes/NA | Geraets et al. 2014 |
| PEGylated Pd nanosheets | 40 nm 86 nm 146 nm | Oral IP | ICR mice | 200 µg/animal | 1 | Up to 8 days | No NM-induced hepatic damage | No pathology | Yes/NA | Chen et al. 2017 |
| BaSO ₄ | ~ 150–350 nm | IT Oral IV | Wistar rats | 1 mg/kg 5 mg/kg 1 mg/kg | 1 | 24 hr | NM accumulation in the liver following IV injection but very little for the other route of exposure | Not analyzed | No | Konduru et al. 2014 |
| C ₆₀ | | IV | ICR mice | 400 µg/animal | 1 | 24 hr | NM accumulation in the liver following IV injection | Not analyzed | No | Wang et al. 2016 |
| Polyurethane | ~ 250 nm | Oral IP | Swiss albino mice | 2, 5 or 10 mg/kg | 1 | Up to 10 days | Increased ALT and inflammatory response – much higher levels following IP exposure | Vascular congestion, vacuolization of hepatocytes and inflammatory cell infiltration | Yes/ Unclear§ | Silva et al. 2016 |

NA – There is no significant initial NM-induced hepatic damage to recover from.

§ – The authors do not state the time-point in which histological analysis was carried out.

comparison to controls mice with regards to an organ-specific inflammatory response, changes in blood biochemistry, acute phase response and hepatic pathology as evidenced by marked changes in intrahepatic architecture, granuloma formation in different zones of the liver, hepatocyte necrosis, parenchymatous degeneration, vacuolar generation and destruction of the liver plates. In addition and most importantly, alcoholic disease markedly influenced and hampered organ ability for recovery post-NM challenge. In the same study, *in vitro* findings demonstrated ethanol pre-treatment of HepG2 cells resulted in significantly increased inflammatory response post-Ag NM exposure. Thus, data indicate the importance of consideration of susceptible individuals in disease liver models in NM risk strategies (Kermanizadeh et al. 2017a).

Lee et al. (2018) administered iv to 6-week-old male Sprague-Dawley rats weighing approximately 250 g either Au NM (approximately 10 nm), a Ag NM (approximately 10 nm) or a mixture of both NM types for a period of 4 weeks (10 or 100 µg/kg/day for the single NM type exposures or 10/10 or 100/100 µg/kg/day for the mixed NM exposures). Data demonstrated that Ag NMs accumulated in a dose-dependent manner in the liver (up to 7958.2 ± 817.9 ng/g of tissue). The hepatic Au concentration increased also in a dose-dependent manner (up to 3563 ± 1310.7 ng/g of tissue). The mixed Au/Ag NM exposure in the organ also enhanced accumulation dose-dependently after 4-week administration, but at a much lower concentrations. Importantly, the Au NM showed bio-persistence and accumulation in liver over a 4-week period following the single exposure. This bioaccumulation was significantly less (almost absent) for the Ag NMs (Lee et al. 2018). This absence of accumulation of hepatic Ag NMs might be partially attributed to the dissolution of materials over a period of 4 weeks.

Further, the bio-distribution of a Zn-labeled CdSe/CdS/ZnS-QDs (50–100 pmol per animal) (11 nm) was investigated in FVB/N mice (gender not disclosed). The animals were exposed to a single dose of the materials for 2 hr and organ distribution determined. Bargheer et al. (2015) noted that liver and spleen were the major organs to take up the QDs, receiving approximately 70%

of the total injected dose. In addition, iv exposure resulted in localization of QDs within KCs and the liver sinusoidal endothelial cells, but not hepatocytes (Bargheer et al. 2015).

Yang et al. (2018a) exposed pregnant Sprague-Dawley rats to a single dose of either 1 or 5 nmol of a carboxyl coated CdSe/ZnS QD (approximately 20 nm) intravenously. The mother and offspring were examined for up to 180 days post exposure. Results showed that QDs primarily accumulated in livers of the dams at 1 day post exposure. However, hematology, biochemistry and histology observations noted limited NM-induced chronic toxicity in the offspring. In the exposed mothers at 24 hr, serum ALT, AST, bilirubin and gamma glutamyl transaminase levels in the high dose group was significantly increased; however, all liver biomarkers of damage returned to background levels by day 10 post injection. Histopathological analysis also demonstrated severe hepatic cellular apoptosis, necrosis, cytolysis, blurred hepatic sinus borderline, as well as a loss of the integrity and morphology of hepatic lobules in exposed animals at day 1 post exposure. Once again, all of these changes had largely resolved by day 18 post exposure (Yang et al. 2018a). Evidence thus indicates the remarkable ability of liver to regenerate. For assessment of “real” hepatic nanotoxicology, this study also demonstrates that a focus on acute responses alone may be misleading, and that inclusion of a recovery period might be significantly informative for both hazard and risk assessment.

In another recent investigation, the toxicity of a SiO₂ NMs (approximately 150 nm) was examined both *in vitro* and *in vivo*. Firstly, male Sprague-Dawley rats were treated iv with 50 mg/kg of SiO₂ NMs and sacrificed at 48 hr after a single dose. Further, buffalo rat liver (BRL) cells were treated with supernatants derived from SiO₂ NM-stimulated KCs (isolated primary cells) (*in vitro* 24 hr exposure at a concentration range of 100–800 µg/ml) to determine KC-mediated hepatotoxicity. Chen, Xue, and Sun (2013) showed as compared with control NMs-induced inflammatory cell infiltration at the portal regions of the liver. In addition, exposure of rats to SiO₂ NMs for 48 hr resulted in a significant rise in the number of KCs in the tissue. Finally, NM exposure produced

an elevation in AST, total bile acid, cholesterol and low-density lipoprotein serum levels in these animals. *In vitro* data observations indicated that NMs induced a concentration-dependent release of hydrogen peroxide (H_2O_2). Further, KCs stimulated with NMs secreted significant quantities of the pro-inflammatory cytokine TNF- α . Chen, Xue, and Sun (2013) also showed that supernatants of the KCs stimulated with SiO_2 NMs, subsequently reduced cellular viability in BRL cells.

The toxicity and bio-distribution of a 50 nm SiO_2 NM was also investigated following a single IV exposure at dose of 20 mg/kg for periods of up to 7 days by Baati et al. (2016). These experiments were carried out by utilization of 4-week-old athymic nude female mice. This is a questionable model for a toxicological study as the animals lack a T lymphocyte population. Baati et al. (2016) detected a threefold increase of Si content in livers of exposed animals 24 hr post-NM administration (106.4 μ g/g). However, the NM liver burden was rapidly degraded and completely cleared within 7 days. Examination of biochemical parameters demonstrated a rise in ALT and catalase activity 3 hr post exposure, which returned to background levels by 24 hr after iv injection. Finally, no NM-induced hepatic histopathological damage was found (Baati et al. 2016).

Zhang et al. (2018) investigated both *in vitro* and *in vivo* hepatotoxicity of a mesoporous SiO_2 NMs (approximately 110 nm). In these experiments, L02 cells (hepatocyte cell line) and 6- to 8-week-old BALB/c mice (wild type, NLRP3^{-/-} and caspase 1^{-/-}) were utilized. In the *in vitro* experiments, hepatic cells were treated with NMs at a concentration range up to 120 μ g/ml for either 24 or 48 hr. For mice, treatment was via iv route with NMs at doses up to 50 mg/kg, on three occasions every other day, over a period of 7 days. Firstly, *in vitro* cytotoxicity data showed a concentration and time-dependent decrease in cell viability. The iv NM exposure resulted in significantly increased serum ALT and AST levels at doses of 25 and 50 mg/kg. In addition, IL-1 β , IL18 and caspase 1 activity in liver homogenates were also significantly elevated in treated animals. However, in NLRP3 and caspase 1 KO mice, liver inflammation and hepatotoxicity observed in the wild type animals was abolished. Taken together, data indicated that SiO_2 NMs triggered liver

inflammation and hepatocyte cell death through NLRP3 inflammasome activation (Zhang et al. 2018).

CD-1 strain male mice (8 weeks) were intravenously exposed iv to polyacrylic acid-coated iron oxide NM (approximately 10 nm) at doses of 8, 20 or 50 mg/kg for 24 hr (Rodrigues et al. 2017). Histologic observations noted no marked changes in cellular structures in both 8 and 20 mg/kg NM-treated animals but in the highest dosed group, 4 of 6 mice had clusters of early necrotic hepatocytes, mainly in the periportal regions. Further, NMs were predominantly visible in KCs macrophages as individual entities. In addition, quantitative analysis of distribution showed a clear dose-related response between dose of NMs and area occupied by KCs loaded with iron (Rodrigues et al. 2017).

The fate of gold/iron oxide hetero-structured NMs (with two different coatings – amphiphilic polymer or PEG) (approximately 100 nm) (dose of 56 μ g iron) was examined over a period of 1 year (1, 7, 30, 95, 180 or 360 days). Eight-week-old female C57/BL6 mice weighing approximately 20 g were administered a single dose iv of the materials. In the liver, regardless of time after injection and nature of material coating, NMs were always found within intracellular vesicles in KCs. Bio-persistent Au materials become more frequent over time within the organ (mostly visible in KCs observed in the form of longer chains, lattices or clusters). It is of interest that hepatic bio-accumulation was increased twofold when polymer coating was used in comparison to the PEG coating. This might be explained by the reduced opsonization and elevated circulation time of PEG-coated NMs (Kolosnjaj-Tabi et al. 2015).

Cai et al. (2016) attempted to evaluate the role of the protein corona in Au NM (nanorods) (approximately 220 nm) induced hepatotoxicity and 6–8 week old CD-1 mice were employed. In this set of trials, NMs were pre-incubated with mouse serum or mouse serum albumin for 24 hr before a single iv injection of 5 mg/kg for periods of either 1, 3, 7 or 28 days. Results showed that pre-incubation with mouse serum significantly elevated accumulation of Au NMs in liver at 1 day post injection (over 80% of the injected NMs were detected in the liver). In addition, clearance of the materials was markedly influenced by the protein corona. It is of interest that the Au NMs were

found exclusively in the KCs. At 3 days post injection, NM treatment was also associated with significantly higher levels of γ -glutamyltransferase, bilirubin and total bile acid compared to controls. Cai et al. (2016) also noted organ-specific increase in glutathione (GSH) and antioxidant enzyme activity in terms of superoxide dismutase (SOD) and glutathione peroxidase (GSH-Px), suggesting NM-induced oxidative hepatic stress. Finally, histopathological analysis showed no obvious tissue abnormalities.

The adverse effects of a Au NM (approximately 15 nm) was assessed in 5- to 6-week-old female BALB/c mice and 5- to 6-week-old female F344 rats. Rodents were exposed to a single iv administration 1000 mg/kg of the NMs for a period of up to 28 days (Bahamonde et al. 2018). No marked alterations were detected in behavior, body weight or serum malondialdehyde (MDA), IL18 and IFN- γ levels in any of the animals. Quantification of Au content in liver rose between 1 and 7 days post-iv administration and remained high in both species for the entirety of the 28 days investigated. The NMs accumulated predominantly in KCs. By day 14 post exposure, Bahamonde et al. (2018) observed the formation of microgranulomas (macrophage clusters containing multinucleated giant cells). It should be noted that the administered NM dose in this study was very high; therefore, a note of caution is required in interpretation of the findings. Finally, 3 of the 19 rats exposed to the NMs died unexpectedly within 24 hr of exposure (Bahamonde et al. 2018).

The organ distribution and toxicity of Au nanoprisms (thin – 10 nm with flat single crystals, with three congruent edge lengths of approximately 150 nm) was investigated following IV exposure in 6-week-old male and female Swiss mice (Pérez-Hernández et al. 2017). The animals were exposed to a single dose of the NMs (6 μ g/per g weight) for 72 hr or 4 months. No significant alterations in blood biochemistry at either time-point were found; however, histological analysis 4 months post exposure showed hepatocytes with enlarged vacuoles and an abundance of KCs with black pigments, which were assumed to be the NMs. Further, Pérez-Hernández et al. (2017) determined the distribution of the NMs and reported 25% of injected dose was present in

liver at 72 hr. At 4 months after exposure, tNMs were still present in liver albeit at reduced quantities (10–15% of the initial injected dose).

In another IV exposure study, Wen et al. (2015) examined the long term *in vivo* bio-distribution of a nano graphene oxide functionalized with poly sodium 4-styrenesulfonate (approximately 700 nm). In these experiments, male BALB/c mice (approximately 25 g) were exposed to NMs at a single dose of 4, 8 or 16 mg/kg of the materials for up to 180 days (1, 7, 14, 28, 90 and 180 days). Wen et al. (2015) detected significant increase in ALT and AST levels on day 1 in the 16 mg/kg group. With the exception of ALT levels in the 16 mg/kg, all parameters returned to background levels on day 90. Histopathological analysis of liver tissues showed characteristic black lesions most notably in the KCs up to day 180.

In an interesting iv study, male C57BL/6 mice, aged 6–8-week-old was exposed to a single dose of lanthanide-based up-conversion NM (approximately 40 nm) for 24 hr at doses of up to 150 mg/kg (Campbell et al. 2018). In these experiments, a group of animals was pre-treated with clodronate liposomes to deplete the KC population. First, hematoxylin and eosin staining depicted that NM exposure led to extensive infiltration of inflammatory cells at the higher doses which was associated with enhanced serum ALT activity. Surprisingly, pathologic changes and elevation of ALT levels were increased in clodronate pre-treated mice suggesting that KCs might protect against lanthanide-based NM-mediated up-conversion of hepatic injury. In this study, Campbell et al. (2018) found vast quantities of NMs located in sinusoids. In the KC depleted livers, NMs were predominantly observed in hepatocytes, supporting the hypothesis that KCs act as a filter to prevent the distribution of NMs to hepatocytes.

Oral route of exposure

Bergin et al. (2016) administered orally to two different Ag NMs (PVP or citrate-stabilized colloidal suspensions with median hydrodynamic diameters of 20 and 110 nm, respectively) at doses of 0.1, 1 or 10 mg/kg daily to male C57BL/6 mice (6-weeks-old) for 3 days. In these experiments, an additional silver acetate exposure group was included as the ionic Ag control. The animals were sacrificed on day 3 or 9

post final Ag NM exposure. Results demonstrated that between 70% and 98% of the administered Ag dose was recovered in feces, while particle size and coating did not significantly influence elimination of the NMs (peak fecal Ag detected 6–9 hr post-administration). Bergin et al. (2016) also showed that 0.5% of total administered dose was detectable in liver, spleen and intestines at 48 hr post final Ag NM administration. Finally, no hepatic histopathology was observed following the acute Ag NM exposure regime.

Subsequently, the potential adverse effects of Ag NM (approximately 10 nm) on pregnant dams and embryo-fetal development after maternal exposure were investigated (Yu et al. 2014). In these set of experiments, mated female Sprague-Dawley rats were orally treated daily from gestational days 6–19 with a dose range of up to 1000 mg/kg. The fetuses were examined for signs of embryotoxic effects after the final day of exposure. Data demonstrated that at doses of 100 mg/kg and above there was a significant decrease in GSH levels and activities of GSH reductase catalase in maternal liver tissue. However, Yu et al. (2014) did not find any developmental toxicity as measured by serum biochemistries, organ weight, gestation index, fetal deaths, sex ratio or morphological alterations of the fetus.

Zinc oxide (ZnO) NMs are considered to exhibit relative rapid dissolution that contributes to the toxicity of nano-sized preparations. Oral exposure of negatively charged ZnO NMs (approximately 30 nm) in 5-week-old male and female Sprague-Dawley rats daily for 90 days (125, 250 or 500 mg/kg) followed by a 14-day recovery period resulted in a dose-dependent accumulation in liver (up to 68.67 ng/g tissue) (Park et al. 2014). Analysis of serum biochemistry showed a fall in total serum protein and albumin levels in male mice treated with the higher doses. However, no marked histopathological abnormalities were detectable in any of the animals.

Recently, Kong et al. (2018) administered orally 50 nm ZnO 2000–10000 mg/kg for 14 days to male and female ICR mice (approximately 20 g). Results demonstrated a LD₅₀ of 5177 mg/kg. The sub-chronic oral exposure of ZnO NMs produced infiltration of inflammatory cells in the portal regions of the examined livers as well as significantly higher serum levels of AST and ALT in these mice. It should be noted that the doses used in

this study are extremely high with little physiological relevance (Kong et al. 2018).

In an interesting and comprehensive study, the influence of co-exposure of two ZnO NMs (either approximately 14 and 60 nm) and lead (Pb) (as a means of assessing potential adverse effects of co-exposure to NMs and heavy metals used in water treatment facilities) was undertaken in 5-week-old male C57BL/6 mice on normal or high-fat diets. Jia et al. (2017) orally exposed mice to NMs (200 mg/kg) or NMs/Pb (200 and 150 mg/kg) daily for a period of 2 weeks. First, it was noted that both Pb and ZnO materials were detectable in the liver. The quantification of NMs or NM/Pb was similar in normal and high-fat animals. However, co-exposure of ZnO NMs with Pb elevated the rate of deposition of hepatic Pb compared to levels of Pb administered alone. The co-administration increased levels of heavy metal deposited in the liver by twofold. Jia et al. (2017) also showed that ZnO NMs or ZnO/Pb exposure of mice receiving a normal diet resulted in negligible pathological damage. However, the same exposures in the high-fat diet mice induced significant liver injury in addition to the diet-induced hepatic steatosis. These animals manifested spotty cell necrosis and a mild vacuolar degeneration. Similarly, a reduction in SOD activity and a rise in MDA content of liver tissue was observed only in the high-fat diet mice after exposure to ZnO and Pb. Evidence indicated that the hepatic toxicity of NMs or co-administration was significantly augmented by preexisting hepatic disease initiated by the diet (Jia et al. 2017).

Shrivastava et al. (2014) orally administered to 6-week-old male Swiss albino mice (25–30 g) a dose of 500 mg/kg of a ZnO (80–100 nm), TiO₂ (50–75 nm) or Al₂O₃ (40–50 nm) for 21 consecutive days. Significantly increased hepatic levels of reactive oxygen species (ROS) were found which were most evident for ZnO NMs. Further, both SOD and catalase activity declined in the liver of exposed mice accompanied by a lack of histopathological alterations in treated animals; however, in the TiO₂-treated group particles were entrapped within the KCs.

In an interesting investigation, the hepatotoxic effects of a silica NM (approximately 15 nm) were examined in normal male Kunming mice or

a fructose-induced metabolic syndrome model (approximately 20 g). Li et al. (2018a) fed mice with either 10 mg/kg of the NMs, 30% fructose or both NMs and fructose daily for a period of 30 days. Histological findings illustrated that in the metabolic syndrome mouse NMs markedly exacerbated hepatocyte ballooning which was accompanied by infiltration of inflammatory cells. Further, Masson staining demonstrated collagen deposition (an indicator of fibrosis). Evidence indicates that silica NM exposure induced increased (and additional) hepatic DNA damage in the metabolic syndrome mice compared to healthy animals (Li et al. 2018a).

Bai et al. (2018) treated orally male ICR mice (approximately 30 g) to three differently sized tin sulfide nanoflower NMs (50, 80 or 200 nm) at doses of 250–1000 mg/kg for 14 consecutive days. Any size associated differences were not observed in hepatic toxicity following exposure to NMs. However, the oral administration of 50 nm NMs at the highest doses elevated serum ALT and AST levels. Further, the expressions of metabolic genes in the liver tissues were altered following exposure to the 50 nm NMs at the highest administered dose. In addition, tissues exposed to 1000 mg/kg of NMs displayed slightly disrupted cellular arrangements, moderate interstitial hyperemia, sporadic and focal infiltration of inflammatory cells and moderate apoptosis in the liver (Bai et al. 2018).

de Carvalho et al. (2018) aimed to investigate the therapeutic effects of a Au NM (approximately 8 nm) in male Wistar rats (300 g) with alcohol and methamphetamine-induced liver injury. The animals were orally treated with three daily doses of Au NMs (181.48, 362.48 or 724.96 µg/kg) one hr before administration of ethanol for 28 days. Data demonstrated that the injured livers exhibited significantly greater myeloperoxidase activity than controls which was attenuated in the Au NM (highest dose) administered animals. Further, Au treatment elevated hepatic GSH levels. The treatment with ethanol and methamphetamine resulted in increased inflammatory response measured in terms of IL-1β and TNF-α. The combined treatment of ethanol, methamphetamine and highest dose of the Au NMs was associated with enhanced IL10 production from the liver. Histopathological analysis livers from diseased animals exhibited fat accumulation,

lymphocyte and neutrophil infiltration, necrosis and steatosis. However, treatment with Au NMs produced reduced histopathological damage in the liver. Finally, evaluation of NF-κB, F4/80, protein kinase B, phosphatidylinositol-4,5-bisphosphate 3-kinase, procollagen III, allograft inflammatory factor 1, extracellular signal-regulated kinases 1/2, transforming growth factor-β, fibroblast growth factor, SOD 1 and GPx 1 genes suggested that NM down-regulated activity of KCs and hepatic stellate cells affecting the profile of their pro-inflammatory cytokines, oxidative stress and fibrosis (de Carvalho et al. 2018).

The toxicity of a TiO₂ NMs (approximately 75 nm) was investigated in 3- and 8-week-old male Sprague-Dawley rats following oral exposure at a dose range up to 200 mg/kg daily for 30 days. Wang et al. (2013) detected in 3-week-old rats histopathologic alterations including edema, hepatic cord disarray, perlobular cell swelling, vacuolization and hydropic degeneration at the highest doses. However, this pathology did not appear in the adult (8 weeks) rat liver with only mild infiltration of mild inflammatory cells observed at the highest dose. In addition, there were significant changes in serum biochemistry relating to liver damage, which again was more apparent in the younger animals (Wang et al. 2013).

The role of gut-derived axis in TiO₂ (30 nm) NM-induced hepatotoxicity was investigated by Chen et al. (2019). Four-week-old Sprague-Dawley rats were administered TiO₂ NMs (29 nm) orally at doses of 2, 10 or 50 mg/kg daily for 90 days. Significantly increased levels of total protein, albumin and globulin were found in 10 or 50 mg/kg TiO₂ NM-exposed animals. In contrast, decreased levels of total bilirubin, ALT and AST were observed in the TiO₂ exposed animals at 90 days. This is indicative that AST and ALT activity measurements might not appropriate for assessment of sub-chronic liver damage. Histological analysis of the treated rat tissue demonstrated fatty degeneration of hepatocytes, which appeared as fat vacuoles. Further, a reduction in the level of GSH was accompanied by an accumulation of hepatic MDA and elevated GSH-Px and SOD activity in NM-exposed animals. Finally, the abundance of *Lactobacillus-reuteri* increased and abundance of *Romboutsia* fell significantly in feces of TiO₂ NM-administered rats. Chen

et al. (2019) argued that the slight hepatotoxicity witnessed following NM exposure may be contributed to alterations in intestinal bacterial species and an imbalance of oxidation/antioxidation.

Finally, oral administration of a halloysite ($\text{Al}_2\text{Si}_2\text{O}_5(\text{OH})_4$) nanotube (average length of approximately 400 nm) was undertaken in a 6–8-week-old Kunming mouse model. Wang et al. (2018b) exposed mice to a dose range of 5–300 mg/kg daily for a period of 30 days. The exposure to the highest dose of the NMs resulted in hydropic degeneration with swelling in the cytoplasm of hepatocytes. In addition to these histopathological alterations, significantly decreased GSH-Px and SOD activity in the high dose exposed animals was noted (Wang et al. 2018b).

Inhalation/intratracheal instillation (IT)/intranasal route of exposure

The bio-distribution of Zn was determined in 5-week-old male C57BL/6 mice after exposure to the NMs (4 hr/day) via a whole-body exposure chamber for 2 weeks (aerosol size distribution 46 ± 1.8 nm; exposure mass concentration 3.6 ± 0.5 mg/m³) or 13 weeks (aerosol size distribution 36 ± 1.8 nm; exposure mass concentration 3.3 ± 0.6 mg/m³). To assess the size distribution of the ZnO NM aerosol, air from the chamber was sampled using a scanning mobility particle sizer spectrometer, while mass concentration of the aerosol in the whole-body chamber was measured gravimetrically. In both studies, mice were necropsied either 1 hr or 3 weeks after the last exposure. Firstly, Adamcakova-Dodd et al. (2014) noted that 100% of the ZnO NMs dissolved within the first 24 hr of mixing in an artificial lysosomal fluid (0.11 M concentration of citric acid). A significant rise in levels of Zn in the liver was found associated with no other indication of toxicity in secondary organs (including liver) of the exposed animals. However, a body weight loss of approximately 2 g was observed after the first week of exposure in the sub-chronic exposed animals (Adamcakova-Dodd et al. 2014).

Smulders et al. (2014) examined the bio-distribution of three “pristine” NMs (TiO_2 – approximately 400 nm; Ag – approximately 90 nm; and SiO_2 – approximately 190 nm) and three aged paints containing NMs in male BALB/c mice (6-week-old). The animals were exposed to

NMs via oropharyngeal aspiration once a week for total of 5 weeks (20 μg NMs per exposure) and sacrificed 2 or 28 days post final administration. Data showed significant increases in the “pristine” Ag and SiO_2 in the liver of treated animals. It is of interest that the hepatic metallic content returned to background levels by 28 days after exposure for Ag NMs but not for Si (Smulders et al. 2014).

A single IT administration of 4 NiO NMs with different physiochemical properties at three doses of up to 6 mg/kg, and for 91 days was carried out in 12-week-old male F344 rats. Shinohara et al. (2017) did not observe any NM, dose or time-dependant alterations in NiO burdens in the livers of exposed animals (although in some rats the Ni levels were higher in treated animals compared to negative group).

The hepatic acute phase response and genotoxic effect of two differently charged TiO_2 NMs (-ve approximately 50 nm; +ve approximately 1500 nm) was investigated following a single IT exposure of 6–7 week old female C57BL/6 mice (Wallin et al. 2017). The animals received NMs at doses of 18, 54 or 162 μg /mouse for 24 hr. Data demonstrated NM-induced hepatic DNA strand breaks for both NMs but there was no consistent pattern in the differences between the two NMs. The hepatic acute phase response was analyzed by measurement of *saa3* mRNA levels and found to be increased dose-dependently 24 hr after exposure for both TiO_2 NMs, but only significant at the highest dose utilized.

The systemic toxicity of three sizes of graphite nanoplates (20 μm lateral, 5 μm lateral, and <2 μm lateral and 8–25 nm) was undertaken in 8-week-old male C57BL/6 mice. The animals received 4 or 40 μg of NMs for 4 hr, 1 day, 7 days, 1 month or 2 months by pharyngeal aspiration. Results showed that levels of acute-phase genes (namely – *amyloid P component (Apcs)*, *serum amyloid A1 (Saa1)*, and *haptoglobin (Hp)*) were elevated in the higher dose groups of the 5 and 20 μm materials. The greatest responses in liver was noted at 4 hr and 1 day post exposure and returned to background levels from day 7 onwards (Roberts et al. 2015).

Finally, Saber et al. (2015) administered to 8-week-old female C57BL/6 mice a single IT dose of 18, 54 or 162 μg of CNT (diameter – approximately 15 nm; length 4 μm) or 54, 162 and 486 μg of sanding dust from an epoxy composite with

(0.2%) or without CNT for periods of up to 28 days. Pulmonary exposure to CNT, reference epoxy or CNT epoxy treatment induced a significant elevation in hepatic *Saa1* expression levels. There were no significant differences in the response between epoxy dusts or CNT. In addition, there was no hepatic DNA strand break for any of the tested materials. The CNT and epoxy dust with CNTs induced histological changes compared to controls predominantly manifested as inflammatory cell infiltrations and small and localized regions of necrosis; however, this pathology was not observed with the epoxy dust without CNT (Saber et al. 2015).

Intraperitoneal (ip) injection

In a study using male Wistar albino rats (10–12 week old), ZnO NMs (approximately 35 nm) administered a daily intraperitoneal (ip) dose of 2 mg/kg for 21 days significant hepatic histopathology alterations predominantly manifested as sinusoidal dilatation, KC hyperplasia, inflammatory cells infiltration, necrosis, hydropic degeneration, hepatocyte apoptosis, anisokaryosis, nuclear membrane irregularity and glycogen content depletion (Almansour et al. 2017). However, the physiological relevance of ip exposure to ZnO NMs is questionable.

The protective role of a Fe₃O₄ NM (approximately 35 nm) in Cd²⁺-mediated toxicity was investigated by Zhang et al. (2016). Male Kunming mice (6–8 weeks) were administered ip Fe₃O₄ NM (30 mg/kg) and CdCl₂ (1 mg/kg) once a day for 7 consecutive days. Data showed that in the material only treated animals, the major % NMs accumulated in liver and spleen. However, in the co-cadmium and NM-exposed group the hepatic Fe levels were significantly lower. Histopathological analysis of the livers of NM-treated mice, demonstrated minor swelling in hepatocytes around the central vein. In the Cd group, hydropic degeneration was prominent with spotty necrosis of hepatocytes. In addition, mesothelial hyperplasia was observed on the liver surface. However, in co-exposure animals, hepatic damage was significantly attenuated. Finally, analysis of serum biochemical parameters revealed that exposure to the NMs alone exerted no marked biological effect in any of the investigated biomarkers of

hepatic damage. In contrast, mice administered CdCl₂ resulted in significant increases in activities of ALT, AST, lactate dehydrogenase (LDH) and levels of total bilirubin (TBIL). Co-exposure attenuated the same hepatic biochemical parameters. Zhang et al. (2016) concluded co-exposure to Fe₃O₄ NMs and CdCl₂ significantly attenuates Cd-induced hepatic damage.

Song et al. (2014) examined the toxicity of anatase TiO₂ nanosheets (92.5 nm) for up to 30 days in 8-week-old C57BL/6 mice following a single ip injection (10 mg/kg). Bio-distribution data showed that 4.32% of administered dose was detected in liver after 24 hr, which was reduced to 4.03% at day 7 and 1.21% by day 30. However, this accumulation was not associated with any significant histopathological damage at any of the time-points investigated.

Swiss albino mice (approximately 35 g) were injected with a single ip dose of a MWCNT (110–170 nm and 5–9 μm length) (1.5, 2 or 2.5 mg/kg) or a mesoporous silica NM (approximately 8 nm) (doses of 10, 25 or 50 mg/kg) for 7 days. Determination of AST, ALT, alkaline phosphatase (ALP) activities and total protein after 7 days resulted only in a significant increase in AST activity following exposure to the MWCNTs (Rawat et al. 2017). This response was not dose dependent. Further, no SiO₂ induced hepatic response was observed in these experiments. It also should be noted that changes in serum biochemistry at peak day 7 post exposure might not be ideal for such measurements.

Dermal route of exposure

The hepatotoxic effects of a dextran-coated ferrite NM (approximately 85 nm) were investigated in a guinea pig (300–350 g) model. The NMs were made into a paste and applied topically on the clipped upper back region of the animals (80 mg/animal). This procedure was repeated three times a week for a period of 3 weeks (a total of 9 doses). Mohanan et al. (2014) demonstrated no significant alterations in oxidative stress, changes in hematology and biochemical parameters or oxidative stress-related DNA damage in the livers of exposed animals.

In an interesting study, C3.Cg/TifBomTac hairless mice (10–15 weeks old) were tattooed with either black or red ink (back of the animal – 1.5×4 cm). These mice were sacrificed after 365 days of being tattooed and distribution to lymph nodes and peripheral organs was examined. Sepehri et al. (2017) showed significant ink pigment deposits in the KCs in 19 of 20 tattooed animals.

Multiple routes of exposure

Ashajyothi, Handral, and Kelmani (2018) examined hepatotoxicity of Cu and ZnO (16–96 nm) NMs following ip or iv administration in a 12–13 week old male Wistar rats. The animals were exposed to the NMs at a dose range of 6.1 to 19.82 $\mu\text{g/kg}$ (Cu NMs) and 11.14 to 30.3 $\mu\text{g/kg}$ (ZnO NMs) (single exposure) for either 14 or 28 days. Data showed that neither ip nor iv administration of the NMs resulted in mortality. However, an elevation in serum creatinine levels, and activities of ALT, AST and ALP was noted following treatment with the highest dose utilized in these experiments. These adverse effects were greater (albeit mild) for ip compared to iv route. Ashajyothi, Handral, and Kelmani (2018) reported toxicity of the ZnO was found to be less than Cu NMs.

In a bio-distribution study, Fu et al. (2013) exposed 6–8 week old female ICR mice to mesoporous silica NMs (110 nm) at a single dose for up to 7 days (24 hr or 7 days) via either iv, hypodermic, intramuscular (im) and oral routes. Results demonstrated that small quantities of the NMs administered im or hypodermic injection localized in liver but with a low absorption rate. Further, with oral administration accumulation and persistence in the liver occurred. As expected, iv exposure resulted in the highest accumulation in liver at 24 hr post-treatment. However, NMs did not induce any marked changes in hepatic appearance and micromorphology at 24 hr or 7 days at a dose of 50 mg/kg (Fu et al. 2013).

In an interesting investigation, Geraets et al. (2014) determined tissue distribution of 5 differently sized JRC TiO₂ NMs in 9- to 10-week-old male and female Wistar rats following either oral or iv treatment (doses of 2.3 mg/rat). The animals were dosed either once or on 5 consecutive days and bio-distribution measured at day 2/6, 14, 30

or 90. Following oral exposure, only small quantities of the Ti was detectable in the livers of treated rats. However, both the single and repeated IV exposure resulted in rapid distribution to the liver. Geraets et al. (2014) found that during the 90 days post exposure period (iv route) only a decrease of approximately 25% was observed for the different TiO₂ NMs. Overall, evidence indicated that NM uptake and distribution combined with slow elimination of NMs might result in potential long-term tissue accumulation.

The oral and ip administration of a polyurethane NM (approximately 250 nm) at doses of 2, 5 or 10 mg/kg in male Swiss albino mice (6–8 week old) for a period of 10 days induced an increase in ALT activity levels (Silva et al. 2016). Further, histopathological examination of the liver of the orally treated mice revealed vascular congestion and vacuolization of hepatocytes, as well as inflammatory infiltrate of exposed animals. Finally, serum IL6 levels were determined and data demonstrated that 5 or 10 mg/kg of NMs ip induced a 40–60 fold-enhanced response. Similarly, following oral administration, IL6 levels were also increased albeit at lower levels compared to ip route. Further (Silva et al. 2016) noted a significant rise in TNF- α levels (approximately 80-fold) in mice administered orally 10 mg/kg NMs.

Engineered NMs and the liver – *in vitro/ex-vivo* studies

Co-culture test model (hepatocytes, KCs and sinusoidal endothelial cells)

In a unique series of *in vitro* studies, a 3D primary human liver spheroid model (compromised of primary human hepatocytes, KCs and hepatic endothelial cells) were exposed to a single or long-term multiple exposure (up to 13 exposures on every other day) of a panel of NMs (Ag – approximately 100 nm, ZnO – approximately 200 nm, MWCNT – D 30 nm, L 700–3000 nm and a positively charged TiO₂ – approximately 250 nm, CeO₂ – approximately 200 nm and DQ12 – approximately 250 nm) for periods of up to 3 weeks which included recovery periods of up to

2 weeks for certain exposure scenarios. The results showed that low dose-repeated exposure to be more damaging to the liver tissue and more severe following treatment with Ag and ZnO NMs in terms of cytotoxicity, cytokine secretion and lipid peroxidation (Kermanizadeh et al. 2019a, 2019b, 2014c). It was found that KCs are crucial in dictating the overall hepatic toxicity following exposure to the materials. Further, findings indicated that *in vitro* AST measurement not to be suitable in a nanotoxicological context. In addition, cytokine analysis (IL6, IL8, IL10 and TNF- α) proved useful in demonstrating recovery periods as being sufficient for enabling a reduction in NM-induced pro-inflammatory responses. Finally, low soluble NM-treated MT displayed a concentration-dependent penetration of materials deep into the tissue (Kermanizadeh et al. 2019a, 2019b, 2014c).

Co-culture test models (hepatocytes and KCs)

In an *in vitro* study, a comparative analysis of the toxicological impact of 29 metal oxide NMs (including cobalt oxide (Co_3O_4), CuO, Fe_3O_4 , antimony oxide (Sb_2O_3), TiO_2 , tungsten trioxide (WO_3), gadolinium oxide (Gd_2O_3) and ZnO) was undertaken by Mirshafiee et al. (2018) in KUP5 (immortalized mice KCs) and Hepa-1-6 cells (mice hepatocyte cell line). In these experiments, both cell types were incubated with a panel of NMs for a period of 24 hr at a concentration range of up to 50 $\mu\text{g}/\text{ml}$. Data demonstrated differences in toxicological profile of metals between hepatocytes and KUP5. The transition-metal oxides induced caspases 3 and 7 activation in both cell types, while rare-earth oxide NMs produced lysosomal damage, NLRP3 inflammasome activation, caspase 1 activation and pyroptosis in KCs but not hepatocytes. The pyroptosis in KUP5 cells was accompanied by cell swelling, membrane blebbing, IL-1 β secretion and increased membrane permeability.

Xue et al. (2014) incubated buffalo rat liver (hepatocytes) or primary rat KC with a 90 nm SiO_2 NM for a period of 24 hr (up to 1000 $\mu\text{g}/\text{ml}$). Exposure of hepatocytes to NMs induced a concentration dependant reduction in cell viability and increased mitochondrial damage. Further, Xue et al. (2014) noted that SiO_2 NMs were potent

inducers of TNF- α and nitric oxide in KCs. Finally, the supernatants from NM-treated KC were transferred to stimulate BRL cells and found to inhibit mitochondrial respiratory chain complex I activity in the hepatocytes.

Co-culture test model (hepatocytes and sinusoidal endothelial cells)

Tee et al. (2019) utilized a 3D co-culture system composed of LO2 cells (hepatic cell line) and primary liver sinusoidal endothelial cells and found that TiO_2 NM (approximately 20 nm) exposure (500 μM 24 hr) diminished the attachment of the endothelial cells onto hepatocytes into the hepatocyte cell line.

Hepatocyte only test models

Recently Ahmed et al. (2017) incubated HepG2 (human hepatocarcinoma) cells to a concentration range up to 100 $\mu\text{g}/\text{ml}$ of 5 differentially coated Ag NMs bis(2-ethylhexyl)-sulfosuccinate (AOTAgNM) (approximately 50 nm), cetrimonium bromide (CTABAgNM) (approximately 75 nm), poly(vinylpyrrolidone) (PVPAgNM) (approximately 60 nm), poly-L-lysine (PLLAgNM) (approximately 90 nm) and bovine serum albumin (BSAAGNM) (approximately 90 nm) for 24 hr. The findings demonstrated concentration-dependent effects on cytotoxicity and genotoxicity in HepG2 cells. The cytotoxic potential of differentially coated Ag NM was listed in the order of BSAAGNM > PLLAgNM > CTABAgNM > AOTAgNM > PVPAgNM. In addition, treatment of HepG2 cells to non-cytotoxic concentrations of the Ag NMs-induced primary DNA damage as evidenced by alkaline comet assay. Finally, Ahmed et al. (2017) showed the principal mechanism for NM uptake was macropinocytosis and clathrin-mediated endocytosis.

In a 24 hr *in vitro* exposure of HepG2 cells to Ag NM (approximately 25 nm), at a concentration range up to 100 $\mu\text{g}/\text{ml}$, the particles produced significant cytotoxicity at concentrations above 5 $\mu\text{g}/\text{ml}$ (Braeuning et al. 2018). Subsequent elemental analysis of Ag in hepatocytes suggested that only a small fraction of Ag was taken up (or

retained) by the cells (8% of administered concentration). Finally, a comprehensive bioinformatics analysis of proteomic data at sub-lethal concentrations showed alterations related to redox stress, mitochondrial dysfunction, intermediary metabolism, inflammatory responses and post-translational protein modifications (Braeuning et al. 2018).

Mishra et al. (2016) used HepG2 cells to investigate the mechanisms underlying toxicity of three differently sized Ag NMs (10, 50 or 100 nm). In these experiments, cells were exposed to low concentrations of the NMs (≤ 10 $\mu\text{g/ml}$). Data demonstrated that NM exposure was associated with induction of the autophagy pathway, enhanced lysosomal activity, increased caspase-3 activity as well as activation of NLRP3-inflammasome. The 10 nm NMs exhibited the highest cellular responses compared with larger particles.

Similarly, Sahu et al. (2016) following 24 hr incubation of HepG2 cells with 20 or 50 nm Ag NMs at a concentration range up to 50 $\mu\text{g/ml}$, the smaller NM-induced micronucleus formation in the cells, while the exposure to the larger particle and ionic control produced a significantly weaker genotoxic response.

Kermanizadeh et al. (2017b) examined the role of autophagy in HepG2 cell death was investigated following exposure to a panel of widely used metallic NMs (Ag – approximately 50 nm; ZnO – approximately 100 nm; and TiO_2 – approximately 150 nm). The cells were exposed to the NMs over several periods up to 24 hr. The time-course investigation of LC3B, atg12, atg3, atg4b, atg5 and p62 genes and proteins and TEM analysis showed that the exposure of the ZnO and Ag NMs resulted in the formation of autophagosomes followed by a blockage of the development of the autolysosome. This response was not observed for the TiO_2 NMs. Further, this dysfunction of the autophagy pathway following exposure to ZnO and Ag NMs preceded apoptotic cell death (flow cytometry analysis, cathepsin B and caspase 3 activity). A number of alterations in the globular-actin networks was observed following exposure to the ZnO and Ag NMs (most evident for the Ag NMs) which appeared more condensed or bundled compared to controls or TiO_2 NM-exposed cells. Evidence indicates involvement of

the cytoskeleton in the blockage of autophagy in the ZnO and Ag NM-treated cells (Kermanizadeh et al. 2017b).

In vitro exposure of HepG2 cells to a collagen-based ZnO NMs (approximately 50 nm) for 24 hr showed NMs to be cytotoxic with an inhibitory concentration 50 (IC_{50}) of 42 $\mu\text{g/ml}$ (Vijayakumar and Vaseeharan 2018).

Wang et al. (2018a) incubated HepG2 cells with three different trifluoroethyl aryl ether-based fluorinated poly (methyl methacrylate) NMs with 5%, 6.1% or 12% fluorine content (all around 600 nm) for a period of 24 hr. All NMs produced cytotoxicity above 100 $\mu\text{g/ml}$ irrespective of fluorine content. The effects of NM exposure on the cell cycle were also investigated. Data showed that in NM-treated cells compared with negative control, the relative % hepatocytes in G0/G1 phase decreased (4.3–6.8%); while cells in the G2/M phase rose (3.3–6.7%), suggesting that the mitotic process was blocked and the cell cycle arrested (Wang et al. 2018a).

In another *in vitro* study, Chevallet et al. (2016) determined the toxic effects of a ZnO NMs (230 nm) in HepG2 cells with a focus on metal homeostasis and redox balance disruptions following exposure to a concentration up to 30 $\mu\text{g/ml}$. A lethal concentration 50% (LC_{50}) of around 20 $\mu\text{g/ml}$ was identified following 24 hr exposure. Zinc homeostasis disruptions were demonstrated as evidenced by an up-regulation of *metallothionein 1X* and *zinc transporter 1* and *2* genes. Further, NM exposure was associated with the induction of oxidative stress response genes (*heme oxygenase 1* and *glutamate-cysteine ligase* were upregulated) (Chevallet et al. 2016).

Thongkam et al. (2017) determined cytotoxicity and genotoxicity of a panel of 10 engineered NMs in HepG2 cells. In these experiments, 5 different TiO_2 , two ZnO, Ag and two MWCNT (panel of NMs in the FP7 funded project ENPRA) were utilized at a concentration of up to 80 $\mu\text{g/cm}^2$ for 24 hr. Data showed Ag and ZnO NM to be highly cytotoxic. Further, DNA damage, as assessed by alkaline comet assay, was only detected with Ag and ZnO, albeit only at cytotoxic concentrations.

In another *in vitro* toxicological study, the human liver cell line (HL-7702) and rat liver cell line (BRL-3A) were exposed to a SiO_2 NMs

(approximately 20 nm) for a period of 72 hr (up to 500 $\mu\text{g/ml}$). Zuo et al. (2016) noted a concentration-dependent toxicity with more severe cytotoxicity in HL-7702 than BRL-3A cells. The increase in intracellular and reduced GSH suggested elevated oxidative stress in both cell types. Western blot analysis revealed that exposure to the SiO_2 NMs resulted in up-regulation of regulated p53, Bax and cleaved caspase-3 as well as a down-regulation of Bcl-2 and caspase-3. Finally, pre-treatment with the antioxidant ascorbic acid significantly attenuated SiO_2 NMs-induced caspase-3 activation.

The *in vitro* hepatic uptake and toxicity of 40 and 80 nm Au NMs modified with polyethyleneimine (BPEI), lipoic acid (LA) and polyethylene glycol (PEG), human plasma protein (HP) and human serum albumin (HSA) coronas was investigated in a primary human hepatocyte model following a 24 hr exposure by Choi, Riviere, and Monteiro-Riviere (2017). Cells were treated with different materials up to a concentration of 125 $\mu\text{g/cm}^2$. From the panel of Au NMs, the BPEI coated NMs induced the highest toxicity with a LC_{50} reached. A time-dependent rise in uptake occurred for all uncoated NMs with the exception of HP and HSA coated particles. Further, a time- and concentration-dependent elevation in ROS/reactive nitrogen species (RNS) was correlated with increasing cytotoxicity at 24 hr post exposure (Choi, Riviere, and Monteiro-Riviere 2017).

Exposure of HepG2 cells to Au nanorods (GNRs) (10 and 25 nm) (10–50 $\mu\text{g/ml}$) for 48 hr resulted in a concentration-dependent toxicity (IC_{50} for 10 nm GNRs, 25 nm GNRs and quartz (positive controls NMs) were 20, 27 and 36 $\mu\text{g/ml}$, respectively) (Lingabathula and Yellu 2016). Incubation with GNRs also resulted in a depletion of intracellular reduced GSH, while TBARS, caspase 3 and IL8 were all elevated.

In vitro exposure of HepG2 cells for 24 hr to 100 $\mu\text{g/ml}$ of covalently conjugated graphene/Au (approximately 13 nm) and graphene/Ag (approximately 50 nm) composites, produced reduced viability to 65% and 60%, respectively (Zhou et al. 2014). In addition, inductively coupled plasma mass spectrometry analysis of intracellular metal content of HepG2 cells after incubation with the GO/NMs composites for 24 hr showed metal content of 40 pg/cell for both NMs.

In a metabolomics study, Kitchin et al. (2014) treated HepG2 cells to a panel of 4 TiO_2 and two CeO_2 NMs at a concentration of 3 or 30 $\mu\text{g/ml}$ for 72 hr. Data demonstrated that five of the NMs markedly depleted reduced GSH with the greatest effects induced by exposures to TiO_2 (59 nm) and CeO_2 (8 nm). In contrast, a 70 nm anatase TiO_2 exerted no significant effect. An addition, CeO_2 , but not TiO_2 , elevated asymmetric dimethylarginine concentrations (involved in cardiovascular disease, diabetes mellitus and kidney disorders).

Recently Bessa et al. (2017) examined the hepatic toxicity of a free rutile TiO_2 NM (approximately 197 nm in medium), nanocomposites of the same TiO_2 (470 nm in medium) and the TiO_2 NMs anchored in nanokaolin clay (447 nm in serum-supplemented medium) using HepG2 cells. Cells were exposed to a concentration range of 5–300 $\mu\text{g/ml}$ for TiO_2 NMs; 45–2700 $\mu\text{g/ml}$ for clay and 50–3000 $\mu\text{g/ml}$ for TiO_2 nanocomposite, for three exposure periods of 3, 6 or 24 hr. A significant decrease in cell viability after exposure to all studied NMs was detected, which was further associated with an increase in HepG2 DNA damage as assessed by the alkaline comet assay. Bessa et al. (2017) suggested that the anchoring of the particular NMs was not associated with decreased toxicity.

Natarajan et al. (2015) exposed primary rat hepatocytes to a concentration range (25–100 ppm) of three different commercially available TiO_2 NMs (P25 – 800 nm; anatase – 700 nm and rutile – 380 nm) for 72 hr. The results showed that LC_{50} values of P25, anatase and rutile TiO_2 NMs were 74.13 ± 9.72 ppm, 58.35 ± 4.76 ppm and 106.81 ± 11.24 ppm, respectively. Further, the three NMs induced a significant loss in hepatocyte functions (albumin and urea production) and a potent oxidative response in hepatocytes (effects most potent for P25).

In an interesting and unique investigation, the total content of titanium and TiO_2 particles was quantified in 15 human livers postmortem. Heringa et al. (2018) reported total Ti content in the liver ranged from 0.02 to 0.09 mg Ti/kg tissue with an average value of 0.04 ± 0.02 mg. Further, TiO_2 particles were detected in 7 of the 15 livers. The smallest detected TiO_2 particle in the tissue was 85 nm; with the number-based TiO_2 particle

size distributions in liver calculated as 85–550 nm (Heringa et al. 2018).

Thai et al. (2016) in a genomic study incubated HepG2 cells with a panel of 6 differently sized TiO₂ NMs (approximately 20–214 nm) for a period of 72 hr at concentrations ranging from (0.3–30 µg/ml). Exposure to NMs-induced alterations in differentially expressed genes related to NRF2-mediated oxidative stress, acute phase response, cholesterol biosynthesis, fatty acid metabolism, apoptosis and stellate cell activation.

KC only test model

The mechanism underlying NM-induced activation of the inflammasome was investigated in a murine KC line. Kojima et al. (2014) employed LPS activated KCs which were exposed to three differently sized Si NMs (approximately 35, 65 and 280 nm) for 24 hr at a concentration range up to 10 µg/cm². IL-1β production (marker of inflammasome activation) was increased in a concentration-dependent manner in LPS-primed KCs cells and the greatest response was to 35 nm Si NMs. This inflammatory response was partially suppressed by antioxidant (ascorbic acid) pre-treatment.

In an interesting study, the ability of KCs for NM uptake was assessed. In this *in vitro* investigation, KCs were exposed to three differently sized PEGylated Au NMs (15, 60 or 100 nm) at a dose of 1×10^{14} nm²/24 plate well for 4 hr. MacParland et al. (2017) demonstrated that NMs were preferentially taken up by KCs that possessed an M2-like phenotype (CD163). It was further postulated that NM uptake selectively impacted the ability of the resident macrophages to produce pro-inflammatory cytokines, without altering cellular viability or phagocytic ability. Further human liver macrophages were far better than circulating the blood monocytes at ingestion of Au NMs. Size effects were not observed.

Discussion

The potential for NMs to translocate to distal organs following a variety of exposure routes is a reality, with the liver shown to accumulate a large proportion of the total or translocated

dose (Antunes et al. 2017; Argueta-Figueroa et al. 2017; Lim et al. 2017). This clearly highlights the necessity for a thorough investigation of the impact of NM exposure to normal liver function. As demonstrated above a large body of toxicology data has been generated for NMs, using a wide variety of test systems, experimental protocols and end-points. It is apparent that all materials are not equally toxic, and these disparities are to a large extent based upon their physicochemical properties and differing experimental designs. Despite this, from the review of available literature, it is clear that developments have been made in identifying the potential nanotoxicological effects on the liver. However, there are still significant knowledge gaps, which require attention to allow for progression of the field and a better understanding of potential adverse effects of NMs on the liver.

Summary of *in vivo* data

A review of the literature clearly indicates that the route of exposure is extremely important in determining the proportion of the NM dose that reaches the liver. Not surprisingly, iv injection of NMs leads to the largest proportion of administered particle dose reaching the organ where over 80% of injected dose was detected at 24 hr post administration (Lee et al. 2018), since there is no barrier to reaching the blood, allowing direct transport of the full dose to the liver sinusoid system. Although, of course, not all of this initial dose will remain as free NMs on reaching the liver. It is also evident that NMs translocate to secondary organs following inhalation and oral administration (Smulders et al. 2014; Zane et al. 2015). Several investigators suggested that the extent of uptake of insoluble NMs from the GIT and airways is in the order of approximately 1–5% of the total applied dose (summarized in Kermanizadeh et al. 2015), detectable in the liver as early as 24 hr post exposure (Gosens et al. 2015; Thakur et al. 2014). However, it is worth noting that data indicate that there are clear differences in biokinetics following exposure to NMs by instillation and inhalation (summarized in Kermanizadeh et al. 2015), which might be explained by local epithelial membrane damage following instillation, which seems to result in increased levels of translocated NMs. Therefore, caution needs to be exercised when extrapolating

data from instillation experiments to the (more representative) inhalation model. A notable number of instillation studies, however, showed systemic translocation, bio-distribution and effects on extra-pulmonary tissues (Gosens et al. 2015; Saber et al. 2015). The vast majority of studies employed metallic elements, metal oxides or organic NMs principally due to the fact that these can be tracked as materials (not elemental ions) in tissue (Gosens et al. 2016; Wallin et al. 2017).

Few studies examined longer-term bio-distribution of NMs, however, interestingly and crucially, data demonstrated that low-solubility materials accumulate in the liver (predominately in KCs), for relatively long periods of time (assessed up to 1 year) (Kolosnjaj-Tabi et al. 2015; Sepehri et al. 2017). This suggests that longer-term consequences of NM exposure need to be considered in the case of liver, especially for those that demonstrate bio-persistence.

In terms of investigations that assessed hepatic hazard of materials, the majority of the NM-induced effects in liver are observed following exposure to high doses (in many instances these are considerably above physiological relevance) (Kumar and Abraham 2016). These effects have been measured, but not limited to, changes in biochemical parameters, antioxidant depletion, genotoxicity and organ pathology, with the extent of adversity varying between different NMs. Inhalation is considered the most important exposure route from an occupational perspective. However, only 4 inhalation study were conducted over the last 5 years in which hepatic effects were determined (Adamcakova-Dodd et al. 2014; Gosens et al. 2016; Guo et al. 2020a; Liu et al. 2019), suggesting that this remains a gap in knowledge. Short term IT studies suggest that NMs have the potential to induce acute impacts on liver mostly notable in terms of changes in serum biochemistry associated with liver damage and DNA damage (Wallin et al. 2017; Yu et al. 2018). However, scrutiny of the data from the few longer-term inhalation/IT studies, seem to indicate that generally speaking acute effects resolve and that this route of exposure only results in relatively non-significant hepatic adverse effects (Adamcakova-Dodd et al. 2014; Smulders et al. 2014).

Oral administration is also conceived as one of the principal routes of human NM exposure, in addition to being the most widely used methodology of

delivering pharmaceuticals. The stability/bio-availability of NMs in the GIT is extremely uncertain due to complexities of the physiology of the stomach and the intestines such as variability of pH in the biological milieu, the presence of the mucus layer and numerous digestive enzymes. This issue is further complicated by the fact that different physicochemical characteristics of varying NMs influence their cellular interactions (Ma et al. 2014). In addition, the physicochemical characteristics of NMs may potentially influence how they are affected in the GIT. From the data published, it was suggested that the extent of NM dissolution might be the decisive factor determining uptake into the body following GIT exposure, and the severity of resulting systemic (including liver) effects (Kong et al. 2018; Patlolla, Hackett, and Tchounwou 2015). Overall, the review of current literature does not enable an accurate estimation of hepatic adverse effects following oral exposure. This being said, from the limited published data it appears that the distribution of NMs to the liver following oral exposure is low (Geraets et al. 2014).

Next, a selected number of *in vivo* studies reported that preexisting disease state of the liver is important not only in augmentation of acute NM-induced damage (manifested a pathological and biochemical changes) and but more importantly hampering the organ's ability for recovery post-NM challenge (Du et al. 2018; Kermanizadeh et al. 2017a). This is of significant importance, as up to 30% of adult population globally suffer from a wide spectrum of sub-clinical often undiagnosed liver damage without any apparent disease manifestations. Therefore, it is critical that liver disease is considered for future hazard and risk assessment strategies for NMs.

From the scrutinization of published data, it is evidently clear that there are no (with the exception of Heringa et al. 2018) epidemiological studies that investigated potential adverse effects of NMs on human liver. Therefore, despite numerous *in vitro* and *in vivo* publications on the subject over the last decade the scientific community is still not that well informed on how NMs actually affect human liver over a life-time. This is of crucial importance for enabling more meaningful hazard assessment strategies but even more essentially as these data would be invaluable to risk assessors.

As a final but important note, a NOAEL level was not included for the studies examined in this review due to the fact that these doses differ depending upon specific toxicological end-point being investigated. This further highlights the absolute necessity to investigate numerous end-points and time-points to enable more useable realistic data for “real” hazard and risk assessment purposes.

Highlights of the progress made in *in vivo* hepatic nanotoxicology 2013–2018

- (1) KCs are the main hepatic cell population relevant for the accumulation of low-solubility NMs (up to months after initial dosing) (Bargheer et al. 2015; Kolosnjaj-Tabi et al. 2015; Rodrigues et al. 2017).
- (2) The bio-distribution of NMs to the liver is not necessarily associated with adverse effects (Feng et al. 2015; Kolosnjaj-Tabi et al. 2015; Talamini et al. 2017)
- (3) In almost all investigations in which a recovery period was included the healthy liver was able to fully recover from NM challenge (irrespective of NM type, dose or route of exposure) – this will be discussed in detail below. To the best of our knowledge, there are only two studies in which there is no full hepatic recovery following a recovery period post-NM exposure (Ni – Magaye et al. 2014; QD – Tang et al. 2017) (highlighted in Table 1). It should be stated that in these two studies manifestations of liver damage was mild.
- (4) The scrutinization of the literature clearly revealed that NM-induced adverse effects in the liver are intensified in the diseased organ. Further, the disease state of the liver might influence and hamper the organ’s ability for recovery post-material challenge (Du et al. 2018; Kermanizadeh et al. 2017a).

Summary of *in vitro* data

Numerous studies attempted to assess the nanotoxicological effects of a wide range of engineered NMs in *in vitro* liver models. By examining the information, these sections aim to establish future

testing strategies to enable more meaningful *in vitro* NM-mediated hepatic toxicity. It is difficult to draw direct comparisons across *in vitro* nanotoxicological studies due to a number of different variables to consider. For example, NMs of the same composition are often different between studies (may vary in physicochemical characteristics such as size, shape, charge, coating) (Carneiro and Barbosa 2016). In addition, the experimental protocols often vary, for example, in the concentrations used, preparation methods of NMs, exposure times, use of cell lines or primary cells, cell numbers, media and the serum protein content employed. Despite these disparities, one ostensible pattern is visible across the experimentations – highly soluble NMs are more toxic than low-solubility materials both in primary and hepatic cell lines *in vitro*. How this relates to *in vivo* responses needs to be further investigated, since *in vitro* soluble compounds are trapped within the exposure vessel, while *in vivo* they diffuse from the site of dissolution, reducing the localized concentration over time. This issue is discussed further below.

As an important side note, over the last few years, a number of *in silico* approaches were used in an attempt to ascertain NM-induced hepatotoxicity *in vitro* including association with up- and down-regulation expression analysis of microarrays (Sooklert et al. 2019), NM-mediated liver genotoxicity (Guo et al. 2020b) or quantitative structure-activity relationship (QSAR) modeling (Fourches et al. 2010). However, *in silico* analysis falls outside the remit of this review and will not be discussed further.

Highlights of the progress made in *in vitro* hepatic nanotoxicology 2013–2018

- (1) Apoptosis and autophagy are important processes in NM-induced cell death in hepatocytes *in vitro* (Kermanizadeh et al. 2017b; Wang et al. 2019)
- (2) There have been significant advances in the development of multi-cellular primary human hepatic models, which incorporate important cell populations that are viable and metabolically active for periods of weeks allowing for long-term low dose and

more physiologically relevant exposure of materials (Kermanizadeh et al. 2019a, 2019b).

Kupffer cells (KC)

KCs are liver resident macrophages that are positioned within the lumen of the sinusoid. Importantly, these cells adhere to the sinusoidal endothelial cells that compose the vessel walls. KCs are the first immune cells in the liver that come in contact with the gut bacteria (Nguyen-Lefebvre and Horuzsko 2015), and any particulate matter transported to the liver via the portal vein. In a healthy liver, KCs play a key role in maintenance of liver immune tolerance (partially due to the exposure to low levels of gut-originated antigens, KCs are in a permanent semi-activated state). However, in pathological conditions, these cells may be activated and fully differentiate into M1-like or M2-like macrophages (Beljaars et al. 2014). Due to their position in the liver sinusoids, these cells are arguably the first and most important cell population that encounter non-soluble particulates reaching the liver. This is one of the reasons, these cells govern the hepatic immune response to particulate challenge. In addition, previous *in vitro* (comparisons made between 3D primary human liver MT composed of hepatocytes only or co-cultures of hepatocytes and KCs) (Kermanizadeh et al. 2019b) and *in vivo* (mice with depleted KC cell population) (Kermanizadeh et al. 2014a) studies clearly demonstrated that the pro/anti-inflammatory response of the healthy liver is governed by the resident macrophages. Due to their location, the KCs intercept and capture materials in the sinusoids, consequently preventing a large proportion of the NM dose diffusing to the hepatocytes. This hypothesis is supported by observations of the internalization of majority of NMs in the resident macrophages *in vivo* (Sepehri et al. 2017; Wen et al. 2015). However, KCs are not likely to be 100% effective at preventing hepatocyte exposure to materials as small NMs might access hepatocytes via open fenestrations in the liver sinusoid endothelial lining.

For this reason, it is highly recommended that KCs are incorporated in next generation *in vitro*

hepatic models intended for hazard assessment. This is even more imperative if the *in vitro* models are intended for utilization as a surrogate for *in vivo* testing (Kermanizadeh et al. 2019a, 2019b). The use of *in vitro* hepatocyte models has been beneficial for the last three decades in research and various application areas. Traditionally, hepatocytes were considered as the most important cell population in the liver for drugs and chemical toxicity screening. This is logical and understandable as drugs and chemical toxicity is mainly dominated by their metabolism, with the metabolic intermediates often being hepatotoxic. However, since bio-persistent NMs are not necessarily metabolized, but rather first interact and/or are internalized by KCs (Aalapati et al. 2014; Shrivastava et al. 2014), the use of hepatocyte only mono-cultures might not be appropriate for particle hepatic toxicity screening. It is also important to consider that numerous investigators demonstrated that only a small proportion of the administered dose of any bio-persistent material reaches the hepatocytes *in vivo* (Sepehri et al. 2017; Wen et al. 2015). From these data, it is clear that KCs are highly involved both in NM-induced hepatic biological responses and in their accumulation.

Meaningful *in vitro* to *in vivo* hepatic comparisons and limitations

Despite the highlighted substantial progress in hepatic *in vitro* test systems over the last 5 years, studies still have certain major limitations, which need to be considered and are discussed below. It is generally acknowledged that it is not always possible to make direct or meaningful comparisons between *in vitro* and *in vivo* hepatic toxicological responses. As with other non-hepatic models systems, one of the key reasons for the lack of comparability between biological responses between *in vitro* and *in vivo* systems is that biological responses may not be similar which can often be explained by the many limitations of traditional mono-cellular *in vitro* test systems (Kermanizadeh et al. 2016).

These confines include lack of cross-talk between different cell types (cellular signaling) and different organs, difficulties in equating dosimetry between *in vitro* and *in vivo* models, difficulty to reproduce environmentally or physiologically relevant routes of exposure,

difficulty to reproduce the exact protein corona, etc.; and difficulties in identifying endpoints *in vitro* that can be measured *in vivo* or vice versa. With respect to the last issue, the key is to identify key biomarkers *in vitro* that might be related to *in vivo* responses. As an example, cytotoxicity measurements *in vitro* are often not sufficient to equate or compare to an *in vivo* response. Of particular importance and unique for the liver, is the necessity for consideration of the inability of *in vitro* models to emulate the liver's unparalleled regeneration capability. The liver's ability to regenerate is essential in disease recovery and in distinguishing the ability of different NMs to induce longer-term harm to the human liver. This consideration of liver recovery therefore needs to be incorporated in future *in vitro* and *in vivo* NM hazard assessment strategies.

In future, assessment of NM-induced cytotoxicity to hepatocytes *in vitro* might be more useful for the identification of sub-lethal doses for further study. Even for simple ranking studies, limitations such as lack of clearance, repeated dose and potential for recovery need to be considered. As an alternative to assessment of cytotoxicity, other meaningful organ-specific relevant toxicological end-points/biomarkers might be cogitated. Some recommendations on this are offered in the following section. Further, from analysis of the literature (and our own work), it is suggested that a note of caution is required to avoid over-emphasis of the significance of a hepatic biological response. As two examples of this: a) an increased cytokine secretion by a hepatocyte cell line *in vitro* might not necessarily equate to a hepatic inflammatory response *in vivo*; b) an analysis of blood biomarkers relating to liver toxicity in isolation (without other additional toxicological end-points) and at single time-point does not equate to liver damage (Yang et al. 2018b).

As described above, the traditional simple *in vitro* models that are widely used may provide some artifacts for NMs that vary in solubility. For example, a 24 hr *in vitro* exposure of C3A cells (derivative of HepG2 cells) or primary hepatocytes to relatively soluble Ag NMs resulted in significant cytotoxicity. In comparison, an iv injection of mice to a relatively high dose of the same Ag NM resulted in acute increased blood biomarkers of

liver damage and severe histopathological damage. Yet 1 week post exposure, serum biochemistries returned to background levels and histopathological damage had completely resolved. In addition, Ag was completely cleared from the organ 1 week post exposure (Kermanizadeh et al. 2012; 2013; Kermanizadeh et al. 2017a; Kermanizadeh et al. Personal communication). For a relatively insoluble TiO₂ NM, minimal toxicity was detected in hepatocytes *in vitro*, along with no marked impact on acute measures of serum biochemistries and histopathology. This was also noted *in vivo* following an *in vivo* iv exposure of mice. However, importantly the TiO₂ NM bio-persisted and was still detectable in the liver several weeks post exposure in experimental rodent models (Kermanizadeh et al. 2012; 2013; Kermanizadeh et al. Personal communication) as well as importantly in human liver postmortem (Heringa et al. 2018).

These simplified comparisons, which accentuate the organ's regeneration ability and importance of a material's bio-persistence, imply that current *in vitro* hepatocyte hazard assessment strategies (including cell death) might not necessarily be meaningful for the prediction of hepatic damage *in vivo*.

Future recommendations

In vitro studies

Based upon the advancements in hepatic nanotoxicology, it is reasonable to state for the majority of NMs studied in the liver, any meaningful NM-induced adverse effects in the liver occurred at acute time points with the potential to resolve (Kermanizadeh et al. 2017a, 2017b; Yang et al. 2018a), and effects of more relevance would only take place after long-term exposure in man (further discussed below). Therefore, it is essential to establish more advanced, physiologically relevant *in vitro* assessment tools for improved prediction of the adverse effects attributed to life-time NM exposure in humans (as discussed above the considerable progress in the development of multi-cellular primary organoids over the last few years has been a great success with this regard). As touched upon above, the

suitability of 24 hr single exposure *in vitro* monocultures of hepatocytes for hazard assessment are questionable. However, these remain a necessity to distinguish between studies attempting to answer specific questions and hazard assessment investigations. Previously Kermanizadeh et al. (2014b) stated that “data suggests that even simple *in vitro* test models (in this instance utilising only a single cell type) can be extremely valuable in predicating the potential liver response *in vivo*.” Having scrutinized the literature over the last 6 years, as well as our own data and all the arguments above it is difficult to still agree with this statement. Therefore, a number of recommendations are offered for progression and improvement of *in vitro* hepatic nanotoxicology:

- (1) The healthy liver’s ability to regenerate and recover cannot be currently replicated, mimicked or reproduced *in vitro*. Therefore, future meaningful *in vitro* toxicological data potentially need to be generated by utilization of low repeated long-term dosing regimens (Kermanizadeh et al. 2019a).
- (2) *In vitro* acute cytotoxicity (measured as cell death or viability) assessment alone are not that useful for hazard ranking of NMs in the liver, as this end-point has little *in vivo* relevance and the findings do not relate to *in vivo* observations. Therefore, identification and investigation of organ-specific sublethal toxicological end-points are more meaningful for forecasting “real” NM-induced *in vivo* hazard. Naturally, cytotoxicity assessments contribute to such studies in order to identify sub-lethal concentrations.
- (3) A distinction is required for analysis and hazard assessment strategies for high vs. low-solubility materials. Importantly, the persistence of low-solubility materials may need to be considered by addressing longer-term effects.
- (4) The inclusion of KCs is critical in the generation of physiologically relevant *in vitro* hepatic nanotoxicology data (Kermanizadeh et al. 2019b).

***In vivo* studies**

Whilst considerable improvement has been made over the last 5 years in terms of more sophisticated and physiologically relevant *in vitro* hepatic models (Bell et al. 2018; Khanal et al. 2019), for now, the use of *in vivo* models appears to be the most appropriate method to gain an accurate and reliable representation of potential human NM hazard. This being said physiologically relevant *in vitro* models are becoming crucial for supplementation and refinement of *in vivo* testing. Further, the ethical implications of any *in vivo* study must be fully considered. Similar to *in vitro* investigations the implementation of the following recommendations might significantly improve the quality and relevance of *in vivo* data for hazard assessment purposes:

- (1) As discussed above, all *in vivo* hepatic hazard assessment studies need to be designed and executed with intermittent repeated dosing and most importantly with recovery periods (Bahamonde et al. 2018; Yang et al. 2018a, 2018b). Such a protocol enables either accumulation or clearance of NMs, manifestation of adverse effects and potential for organ recovery to be identified, leading to a more realistic understanding of the toxic potential of NMs.
- (2) As for other substances, NM-induced effects should not be overstated. For example, changes in blood biochemistry or redox status at a single time-point are not necessarily representative of pathophysiological liver toxicity (Baati et al. 2016; Park et al. 2014). To this end, the investigation of a wider range of time-points post-material exposure would be beneficial to assess either recovery or disease development. This would also enable the identification of optimum epochs for different end-points.
- (3) A thorough understanding of liver physiology is important in design of a high-quality hepatic nanotoxicology investigation. This will allow for identification of relevant end-points and time-points for an accurate identification of “real” hepatic damage. As an

example, serum ALT and AST activity levels only reflect acute liver injury and are usually lower in chronic liver injury. Therefore, analysis of serum biomarkers after weeks of NM exposure might not be entirely relevant or informative.

- (4) The liver is constantly bombarded with foreign antigens from the gut; therefore, the organ tolerance is manifested as a bias toward immune unresponsiveness (Crispe 2014). This factor needs to be considered in the analysis of certain organ-specific toxicological end-points (e.g. inflammation).
- (5) It has been reported that NM-induced adverse effects in the organ are exaggerated in the diseased liver (Du et al. 2018; Kermanizadeh et al. 2017a). Moreover, disease might affect and hamper the organ's recovery and regeneration post xenobiotic exposure. As discussed above an important and additional complication is that an estimated 25% of the adult general population globally suffer from a spectrum of sub-clinical liver damage. Therefore, it is critical that a range of liver diseases (mild to severe) be considered for inclusion in future NM hazard and risk assessment strategies.
- (6) It is imperative that distribution and toxicity assessments are integrated in future *in vivo* experiments (ideally over time). It is not sufficient to demonstrate accumulation of NMs without the analysis of possible NM-induced effects. As discussed above accumulation does not necessarily equate to adverse effects and vice versa.
- (7) As highlighted few studies examined effects of NMs on the liver following inhalation exposure (in all reality one of the two most prominent routes of NM exposure). Despite the technical, ethical and financial difficulty associated with experiments of this nature, these studies are urgently needed for the progression of hepatic nanotoxicology.
- (8) Studies need to consider the incorporation of multiple appropriate end-points to enable assessment of "real" hazard (with analysis of biochemistry, organ-specific inflammation and histopathology highly recommended)

In order to carry out a well-informed, evidence-based risk assessment for the emerging NMs, a thorough understanding of all aspects of NM risk is required and an important component to achieving this is the design of physiologically relevant test systems and experiments. Further, a critical risk assessment requires knowledge regarding the level of exposure to the manufactured NM, route of exposure, bio-persistence in the organism and inherent toxicity of the material in question. In addition, specific to the liver toxicology is the organs regeneration capability, which needs to be incorporated and considered for all *in vitro* and *in vivo* hazard assessment experiments.

Disclosure statement

The authors have sole responsibility for the writing and content of the paper. The review was prepared as part of their normal work. The strategy for the literature review, the evaluation of the literature and the conclusions drawn and recommendations made are the exclusive professional work of the authors. None of the authors has any actual or potential competing financial interests.

Funding

This work has been financially supported by H2020 funded project PATROLS [Grant code - 760813].

ORCID

Ali Kermanizadeh  <http://orcid.org/0000-0002-2989-9078>

References

- Aalapati, S., S. Ganapathy, S. Manapuram, G. Anumolu, and B. M. Prakya. 2014. Toxicity and bio-accumulation of inhaled cerium oxide nanoparticles in CD1 mice. *Nanotoxicology* 8:786–98. doi:10.3109/17435390.2013.829877.
- Abbasalipourkabir, R., H. Moradi, S. Zarei, S. Asadi, A. Salehzadeh, A. Ghafourikhosroshahi, and M. Mortazavi. 2015. Toxicity of zinc oxide nanoparticles on adult male Wistar rats. *Food Chem Toxicol* 84:154–60. doi:10.1016/j.fct.2015.08.019.
- Adamcukova-Dodd, A., L. V. Stebounova, J. S. Kim, S. U. Vorrink, A. P. Ault, P. T. O'Shaughnessy, V. H. Grassian, and P. S. Thorne. 2014. Toxicity assessment of zinc oxide nanoparticles using sub-acute and sub-chronic murine inhalation models. *Part Fibre Toxicol* 11:15. doi:10.1186/1743-8977-11-15.

- ADC, M., L. F. Azevedo, C. C. D. S. Rocha, M. F. H. Carneiro, V. P. Venancio, M. R. de Almeida, L. M. G. Antunes, R. D. C. Hott, J. L. Rodrigues, A. T. Ogunjimi, et al. 2017. Evaluation of distribution, redox parameters, and genotoxicity in Wistar rats co-exposed to silver and titanium dioxide nanoparticle. *J Toxicol Env Health A* 80:1156–65. doi:10.1080/15287394.2017.1357376.
- Ahmed, L. B., M. Milic, I. M. Pongrac, A. M. Marjanovic, H. Mlinaric, I. Pavicic, S. Gajovic, and I. V. Vrcck. 2017. Impact of surface functionalization on the uptake mechanism and toxicity effects of silver nanoparticles in HepG2 cells. *Food Chem Toxicol* 107:349–61. doi:10.1016/j.fct.2017.07.016.
- Al-Badri, A. M., A. F. Bargooth, J. G. Al-Jebori, and E. A. K. Zegver. 2019. Identification of carbon nanotubes in liver tissue and its effects on apoptosis of birds exposed to air pollution. *Vet World T* 12:1372–77. doi:10.14202/vetworld.2019.1372-1377.
- Almansour, M. I., M. A. Alferah, Z. A. Shraideh, and B. M. Jarrard. 2017. Zinc oxide nanoparticles hepatotoxicity: Histological and histochemical study. *Environ Toxicol Pharmacol* 51:124–30. doi:10.1016/j.etap.2017.02.015.
- Antunes, A. F., P. Pereira, C. Reis, P. Rijo, and C. Reis. 2017. Nanosystems for skin delivery: From drugs to cosmetics. *Curr Drug Metab* 18:412–25. doi:10.2174/1389200218666170306103101.
- Argueta-Figueroa, L., O. Martinez-Alvarez, J. Santos-Cruz, R. Garcia-Contreras, L. S. Acosta-Torres, J. de la Fuente-hernandez, and M. C. Arenas-Arrocena. 2017. Nanomaterials made of non-toxic metallic sulfides: A systematic review of their potential biomedical applications. *Mater Sci Eng C Mater Biol Appl* 76:1305–15. doi:10.1016/j.msec.2017.02.120.
- Ashajyothi, C., H. K. Handral, and C. R. Kelmani. 2018. A comparative *in vivo* scrutiny of biosynthesized copper and zinc oxide nanoparticles by intraperitoneal and intravenous administration routes in rats. *Nanoscale Res Lett* 13 (1):93. doi:10.1186/s11671-018-2497-2.
- Awasthi, K. K., A. Awasthi, R. Verma, I. Soni, K. Awasthi, and P. J. John. 2015. Silver nanoparticles and carbon nanotubes induced DNA damage in mice evaluated by single cell gel electrophoresis. *Macromol Symp* 357:210–17. doi:10.1002/masy.201500018.
- Baati, T., A. Al-Kattan, M. A. Esteve, L. Njim, Y. Ryabchikov, F. Chaspoul, M. Hammami, M. Sentis, A. V. Kabashin, and D. Braguer. 2016. Ultrapure laser-synthesized Si-based nanomaterials for biomedical applications: *In vivo* assessment of safety and biodistribution. *Nature Sci Rep* 6:25400. doi:10.1038/srep25400.
- Bahamonde, J., B. Brenseke, M. Y. Chan, R. D. Kent, P. J. Vikesland, and M. R. Prater. 2018. Gold nanoparticle toxicity in mice and rats: Species differences. *Toxicol Pathol* 46:431–43. doi:10.1177/0192623318770608.
- Bai, D., Q. Li, Y. Xiong, C. Wang, P. Shen, L. Bai, L. Yuan, and P. Wu. 2018. Hepatic, metabolic, and toxicity evaluation of repeated oral administration of SnS₂ nano-flowers in mice. *Toxicol Sci* 164:501–11. doi:10.1093/toxsci/kfy104.
- Bailly, A. L., F. Correard, A. Popov, G. Tselikov, F. Chaspoul, R. Appay, A. Al-Kattan, A. V. Kabashin, D. Braguer, and M. A. Esteve. 2019. *In vivo* evaluation of safety, biodistribution and pharmacokinetics of laser synthesized gold nanoparticles. *Sci Rep* 9:12890. doi:10.1038/s41598-019-48748-3.
- Balasubramanian, S. K., J. Jittiwat, J. Manikandan, C. N. Ong, L. E. Yu, and W. Y. Ong. 2010. Biodistribution of gold nanoparticles and gene expression changes in the liver and spleen after intravenous administration in rats. *Biomaterials* 31:2034–42. doi:10.1016/j.biomaterials.2009.11.079.
- Bargheer, D., A. Giemsa, B. Freund, M. Heine, C. Waurisch, G. M. Stachowski, S. G. Hickey, A. Eychmüller, J. Heeren, and P. Nielsen. 2015. The distribution and degradation of radiolabeled superparamagnetic iron oxide nanoparticles and quantum dots in mice. *Beilstein J Nanotechnol* 6:111–23. doi:10.3762/bjnano.6.11.
- Beljaars, L., M. Schippers, C. Reker-Smit, F. O. Martinez, L. Helming, K. Poelstra, and B. N. Melgert. 2014. Hepatic localization of macrophage phenotypes during fibrogenesis and resolution of fibrosis in mice and humans. *Front Immunol* 5:30. doi:10.3389/fimmu.2014.00430.
- Bell, C. C., A. C. A. Dankers, V. M. Lauschke, R. Sison-Young, R. Jenkins, C. Rowe, C. E. Goldring, K. Park, S. L. Regan, T. Walker, et al. 2018. Comparison of hepatic 2D sandwich cultures and 3D spheroids for long-term toxicity applications: A multicentre study. *Toxicol Sci* 162:655–66. doi:10.1093/toxsci/kfx289.
- Bergin, I. L., L. A. Wilding, M. Morishita, K. Walacavage, A. P. Ault, J. L. Axson, D. I. Stark, S. A. Hashway, S. S. Capracotta, P. R. Leroueil, et al. 2016. Effects of particle size and coating on toxicologic parameters, fecal elimination kinetics and tissue distribution of acutely ingested silver nanoparticles in a mouse model. *Nanotoxicology* 10:352–60. doi:10.3109/17435390.2015.1072588.
- Bessa, M. J., C. Costa, J. Reinosa, C. Pereira, S. Fraga, J. Fernández, M. A. Bañares, and J. P. Teixeira. 2017. Moving into advanced nanomaterials. Toxicity of rutile TiO₂ nanoparticles immobilized in nanokaolin nanocomposites on HepG2 cell line. *Toxicol Appl Pharmacol* 316:114–22. doi:10.1016/j.taap.2016.12.018.
- Bollu, V. S., G. Soren, K. Jamil, A. Bairi, and S. Yashmaina. 2016. Genotoxic and histopathological evaluation of zinc oxide nanorods *in vivo* in Swiss albino mice. *J Evol Med Dent Sci* 5:6186–92. doi:10.14260/jemds/2016/1398.
- Bottcher, J. P., P. A. Knolle, and D. Stabenow. 2011. Mechanisms balancing tolerance and immunity in the liver. *Dig Dis* 29:384–90. doi:10.1159/000329801.
- Boudard, D., F. Aureli, B. Laurent, N. Sturm, A. Raggi, E. Antier, L. Lakhdar, P. N. Marche, M. Cottier, F. Cubadda, et al. 2019. Chronic oral exposure to synthetic amorphous silica (NM-200) in renal and liver lesions in mice. *Kidney Int Rep* 4:1463–71. doi:10.1016/j.ekir.2019.06.007.

- Braeuning, A., A. Oberemm, J. Görte, L. Böhmert, S. Juling, and A. Lampen. 2018. Comparative proteomic analysis of silver nanoparticle effects in human liver and intestinal cells. *J Appl Toxicol* 38:638–48. doi:10.1002/jat.3568.
- Brown, A. L., M. P. Kai, A. N. DuRoss, G. Sahay, and C. Sun. 2018. Biodistribution and toxicity of micellar platinum nanoparticles in mice via intravenous administration. *Nanomaterials* 8:410. doi:10.3390/nano8060410.
- Cai, H., Y. Ma, Z. Wu, Y. Ding, P. Zhang, X. He, J. Zhou, Z. Chai, and Z. Zhang. 2016. Protein corona influences liver accumulation and hepatotoxicity of gold nanorods. *NanoImpact* 3:40–46. doi:10.1016/j.impact.2016.09.005.
- Campbell, F., F. L. Bos, S. Sieber, G. A. Alpizar, B. E. Kocj, J. Huwyler, A. Kros, and J. Russmann. 2018. Directing nanoparticle biodistribution through evasion and exploitation of Stab2-dependent nanoparticle uptake. *ACS Nano* 12:2138–50. doi:10.1021/acsnano.7b06995.
- Canli, E. G., C. Gumus, M. Canli, and H. B. Ila. 2020. The effects of titanium nanoparticles on enzymatic and non-enzymatic biomarkers in female Wistar rats. *Drug Chem Toxicol* 3:1–19. doi:10.1080/01480545.2019.1708925.
- Carneiro, M. F. H., and J. F. Barbosa. 2016. Gold nanoparticles: A critical review of therapeutic applications and toxicological aspects. *J Toxicol Environ Health B* 19:129–48. doi:10.1080/10937404.2016.1168762.
- Chen, Q., Y. Xue, and J. Sun. 2013. Kupffer cell-mediated hepatic injury induced by silica nanoparticles *in vitro* and *in vivo*. *Int J Nanomedicine* 8:1129–40. doi:10.2147/IJN.S42242.
- Chen, X., J. Li, Y. Huang, J. Wei, D. Sun, and N. Zheng. 2017. The biodistribution, excretion and potential toxicity of different-sized Pd nanosheets in mice following oral and intraperitoneal administration. *Biomater Sci* 5:2448. doi:10.1039/C7BM00769H.
- Chen, Z., D. Zhou, S. Han, S. Zhou, and G. Jia. 2019. Hepatotoxicity and the role of the gut-liver axis in rats after oral administration of titanium dioxide nanoparticles. *Part Fibre Toxicol* 16:48. doi:10.1186/s12989-019-0332-2.
- Chevallet, M., B. Gallet, A. Fuchs, P. H. Jouneau, K. Um, E. Mintza, and I. Michaud-Soret. 2016. Metal homeostasis disruption and mitochondrial dysfunction in hepatocytes exposed to sub-toxic doses of zinc oxide nanoparticles. *Nanoscale* 8:18495. doi:10.1039/C6NR05306H.
- Choi, J., H. Kim, P. Kim, E. Jo, H. M. Kim, M. Y. Lee, S. M. Jin, and L. Park. 2015. Toxicity of zinc oxide nanoparticles in rats treated by two different routes: Single intravenous injection and single oral administration. *J Toxicol Env Health A* 78:226–43. doi:10.1080/15287394.2014.949949.
- Choi, K., J. E. Riviere, and N. A. Monteiro-Riviere. 2017. Protein corona modulation of hepatocyte uptake and molecular mechanisms of gold nanoparticle toxicity. *Nanotoxicology* 11:64–75. doi:10.1080/17435390.2016.1264638.
- Crispe, I. N. 2014. Immune tolerance in liver disease. *Hepatology* 60:2109–2017. doi:10.1002/hep.27254.
- de Carvalho, T. G., V. B. Garcia, A. A. de Araújo, L. H. da Silva Gasparotto, H. Silva, G. C. B. Guerra, E. de Castro Miguel, R. F. de Carvalho Leitão, D. V. da Silva Costa, L. J. Cruz, et al. 2018. Spherical neutral gold nanoparticles improve anti-inflammatory response, oxidative stress and fibrosis in alcohol-methamphetamine-induced liver injury in rats. *Int J Pharm* 548:1–14. doi:10.1016/j.ijpharm.2018.06.008.
- Du, L. J., K. Xiang, J. H. Liu, Z. M. Song, Y. Liu, A. Cao, and H. Wang. 2018. Intestinal injury alters tissue distribution and toxicity of ZnO nanoparticles in mice. *Toxicol Lett* 295:74–85. doi:10.1016/j.toxlet.2018.05.038.
- El-Ghor, A. A., M. M. Noshay, A. Galal, and H. R. H. Mohamed. 2014. Normalization of nano-sized TiO₂-induced clastogenicity, genotoxicity and mutagenicity by Chlorophyllin administration in mice brain, liver, and bone marrow cells. *Toxicol Sci* 142:21–32. doi:10.1093/toxsci/kfu157.
- EU commission recommendation. 2011. <https://eur-lex.europa.eu/legal-content/EN/TXT/PDF/?uri=CELEX:32011H0696&from=EN>.
- Fatima, R., and R. Ahmad. 2019. Hepatotoxicity and chromosomal abnormalities evaluation due to single and repeated oral exposures of chromium oxide nanoparticles in Wistar rats. *Toxicol Ind Health* 35:548–57. doi:10.1177/0748233719863632.
- Feng, W., W. Nie, Y. Cheng, X. Zhou, L. Chen, K. Qiu, Z. Chen, M. Zhu, and C. He. 2015. *In vitro* and *in vivo* toxicity studies of copper sulfide nanoplates for potential photothermal applications. *Nanomedicine* 11:901–12. doi:10.1016/j.nano.2014.12.015.
- Fourches, D., D. Pu, C. Tassa, R. Weissleder, S. Y. Shaw, R. J. Mumper, and A. Tropsha. 2010. Quantitative nanostructure-activity relationship modeling. *ACS Nano* 4:5703–12. doi:10.1021/nn1013484.
- Fu, C., T. Liu, L. Li, H. Liu, D. Chen, and F. Tang. 2013. The absorption, distribution, excretion and toxicity of mesoporous silica nanoparticles in mice following different exposure routes. *Biomaterials* 34:2565–75. doi:10.1016/j.biomaterials.2012.12.043.
- Gagne, F., J. A. Auclair, M. Fortier, A. Bruneau, M. Fournier, P. Turcotte, M. Pilote, and C. Gagnon. 2013. Bioavailability and immunotoxicity of silver nanoparticles to the freshwater mussel *Elliptio complanta*. *J Toxicol Env Health A* 76:767–77. doi:10.1080/15287394.2013.818602.
- Gao, M. L., M. T. Lv, U. Liy, and Z. G. Song. 2018. Transcriptome analysis of the effects of Cd and nanomaterial-loaded Cd on the liver in zebrafish. *Ecotoxicol Environ Saf* 164:530–39. doi:10.1016/j.ecoenv.2018.08.068.
- Geraets, L., A. G. Oomen, P. Krystek, N. R. Jacobsen, H. Wallin, M. Laurentie, H. W. Verharen, E. F. A. Brandon, and W. H. de Jong. 2014. Tissue distribution and elimination after oral and intravenous administration of different titanium dioxide nanoparticles in rats. *Part Fibre Toxicol* 11:30. doi:10.1186/1743-8977-11-30.
- Godoy, P., N. J. Hewitt, U. Albrecht, M. E. Andersen, N. Ansari, S. Bhattacharya, J. H. Bode, J. Bolleyn, C. Borner, J. Bottger, et al. 2014. Recent advances in 2D and 3D *in vitro* systems using primary hepatocytes,

- alternative hepatocyte sources and non-parenchymal liver cells and their use in investigating mechanisms of hepatotoxicity, cell signalling and ADME. *Arch Toxicol* 87:1315–530.
- Gosens, I., A. Kermanizadeh, N. R. Jacobsen, A. G. Lenz, B. Bokkers, W. H. de Jong, P. Krystek, L. Tran, V. Stone, H. Wallin, et al. 2015. Comparative hazard identification by a single dose lung exposure of zinc oxide and silver nanomaterials in mice. *PLoS ONE* 10:e0126934. doi:10.1371/journal.pone.0126934.
- Gosens, I., F. R. Cassee, M. Zanella, L. Manodori, A. Brunelli, A. L. Costa, B. G. H. Bokkers, W. H. de Jong, D. Brown, D. Hristozov, et al. 2016. Organ burden and pulmonary toxicity of nano-sized copper (II) oxide particles after short-term inhalation exposure. *Nanotoxicology* 10:1084–95. doi:10.3109/17435390.2016.1172678.
- Guichard, Y., M. A. Maire, S. Sebillaud, C. Fontana, C. Langlais, J. C. Micillino, C. Darne, J. Roszak, M. Stepnik, V. Fessard, et al. 2015. Genotoxicity of synthetic amorphous silica nanoparticles in rats following short-term exposure, part 2: Intratracheal instillation and intravenous injection. *Environ Mol Mutagen* 56:228–44. doi:10.1002/em.21928.
- Guo, X., J.-E. Seo, Z. Li, and N. Mei. 2020b. Genetic toxicity assessment using liver cell models: Past, present and future. *J Toxicol Environ Health B* 23:27–50. doi:10.1080/10937404.2019.1692744.
- Guo, Z., Y. Luo, P. Zhang, A. J. Chetwynd, H. Q. Xie, F. A. Monikh, W. Tao, C. Xie, Y. Liu, L. Xu, et al. 2020a. Deciphering the particle specific effects on metabolism in rat liver and plasma from ZnO nanoparticles versus ionic Zn exposure. *Environ Int* 136:105437. doi:10.1016/j.envint.2019.105437.
- Hanini, A., M. El Massoudi, K. K. Gavard, S. Ammar, and O. Souilem. 2016. Nanotoxicological study of polyol-made cobalt-zinc ferrite nanoparticles in rabbit. *Environ Toxicol Pharmacol* 45:321–27. doi:10.1016/j.etap.2016.06.010.
- Hendrickson, O. D., O. V. Morozova, A. V. Zherdev, A. I. Yaropolov, S. G. Klochkov, S. O. Bachurin, and B. B. Dzantiev. 2015. Study of distribution and biological effects of fullerene C 60 after single and multiple intragastrical administrations to rats. *Fuller Nanotub Car Nanostructures* 23:658–68. doi:10.1080/1536383X.2014.949695.
- Heringa, M. B., R. J. B. Peters, R. L. A. W. Bleys, M. K. van der Lee, P. C. Tromp, P. C. E. van Kesteren, J. C. H. van Eijkeren, A. K. Undas, A. G. Oomen, and H. Bouwmeester. 2018. Detection of titanium particles in human liver and spleen and possible health implications. *Part Fibre Toxicol* 15:15. doi:10.1186/s12989-018-0251-7.
- Hernandez-Moreno, D., A. Valdehita, E. Conde, I. Rucandio, J. M. Navas, and M. L. Fernandez-Cruz. 2019. Acute toxic effects caused by the co-exposure of nanoparticles of ZnO and Cu in rainbow trout. *Sci Total Environ* 687:24–33. doi:10.1016/j.scitotenv.2019.06.084.
- Isoda, K., R. Nagata, T. Hasegawa, Y. Taira, I. Taira, Y. Shimizu, K. Isama, T. Nishimura, and I. Ishida. 2017. Hepatotoxicity and drug/chemical interaction toxicity of nanoclay particles in mice. *Nanoscale Res Lett* 12:199. doi:10.1186/s11671-017-1956-5.
- Jia, J., F. Li, S. Zhai, H. Zhou, S. Liu, G. Jiang, and B. Yan. 2017. Susceptibility of overweight mice to liver injury as a result of the ZnO nanoparticle-enhanced liver deposition of Pb²⁺. *Environ Sci Technol* 51:1775–84. doi:10.1021/acs.est.6b05200.
- Johnston, H., D. Brown, A. Kermanizadeh, E. Gubbins, and V. Stone. 2012. Investigating the relationship between nanomaterial hazard and physicochemical properties: Informing the exploitation of nanomaterials with therapeutic and diagnosis applications. *J Control Release* 164:307–13. doi:10.1016/j.jconrel.2012.08.018.
- Kermanizadeh, A., B. K. Gaiser, G. R. Hutchison, and V. Stone. 2012. An *in vitro* liver model - Assessing oxidative stress and genotoxicity following exposure of hepatocytes to a panel of engineered nanomaterials. *Part Fibre Toxicol* 9:28. doi:10.1186/1743-8977-9-28.
- Kermanizadeh, A., B. K. Gaiser, H. Johnston, D. M. Brown, and V. Stone. 2014b. Toxicological effect of engineered nanomaterials on the liver. *Br J Pharmacol* 171:3980–87. doi:10.1111/bph.12421.
- Kermanizadeh, A., B. K. Gaiser, M. B. Ward, and V. Stone. 2013. Primary human hepatocytes versus hepatic cell line: Assessing their suitability for *in vitro* nanotoxicology. *Nanotoxicology* 7 (7):1255–71. doi:10.3109/17435390.2012.734341.
- Kermanizadeh, A., C. Chauche, D. Balharry, D. M. Brown, N. Kinase, J. Boczkowski, S. Lanone, and V. Stone. 2014a. The role of Kupffer cells in the hepatic response to silver nanoparticles. *Nanotoxicology* 8:149–54. doi:10.3109/17435390.2013.866284.
- Kermanizadeh, A., D. Balharry, H. Wallin, S. Loft, and P. Møller. 2015. Nanomaterial translocation - the biokinetics, tissue accumulation, toxicity and fate of materials in secondary organs - a review. *Crit Rev Toxicol* 45 (10):837–72. doi:10.3109/10408444.2015.1058747.
- Kermanizadeh, A., D. M. Brown, W. Moritz, and V. Stone. 2019b. The importance of inter-individual Kupffer cell variability in the governance of hepatic toxicity in a 3D primary human liver microtissue model. *Nature Sci Rep* 9:7295. doi:10.1038/s41598-019-43870-8.
- Kermanizadeh, A., I. Gosens, L. MacCalman, H. Johnston, P. H. Danielsen, N. R. Jacobsen, A. G. Lenz, T. Fernandes, R. P. F. Schins, F. R. Cassee, et al. 2016. A multilaboratory toxicological assessment of a panel of 10 engineered nanomaterials to human health - ENPRA project - the highlights, limitations, and the current and future challenges. *J Toxicol Environ Health B* 19:1–28. doi:10.1080/10937404.2015.1126210.
- Kermanizadeh, A., K. Jantzen, M. B. Ward, J. A. Durhuus, L. J. Rasmussen, S. Loft, and P. Møller. 2017b. Nanomaterial-induced cell death in pulmonary and hepatic cells following exposure to three different metallic materials: The role of autophagy and apoptosis. *Nanotoxicology* 11:184–200. doi:10.1080/17435390.2017.1279359.
- Kermanizadeh, A., L. Powell, V. Stone, and P. Møller. 2018. Nano delivery systems and stabilized solid drug

- nanoparticles for orally administered medicine - current landscape. *Int J Nanomedicine* 13:7575–605. doi:10.2147/IJN.S177418.
- Kermanizadeh, A., M. Løhr, M. Roursgaard, S. Messner, P. Gunness, J. M. Kelm, P. Møller, V. Stone, and S. Loft. 2014c. Hepatic toxicology following single and multiple exposure of engineered nanomaterials utilising a novel primary human 3D liver microtissue model. *Part Fibre Toxicol* 11:56. doi:10.1186/s12989-014-0056-2.
- Kermanizadeh, A., N. R. Jacobsen, M. Roursgaard, S. Loft, and P. Møller. 2017a. Hepatic hazard assessment of silver nanoparticle exposure in healthy and chronically alcohol fed mice. *Toxicol Sci* 158:176–87. doi:10.1093/toxsci/kfx080.
- Kermanizadeh, A., T. Berthing, E. Guźniczak, M. Wheeldon, G. Whyte, U. Vogel, W. Moritz, and V. Stone. 2019a. Assessment of nanoparticle-induced hepatotoxicity using a 3D human primary multi-cellular microtissue exposed repeatedly over 21 days - suitability of the *in vitro* test system as an *in vivo* surrogate. *Part Fibre Toxicol* 16:42. doi:10.1186/s12989-019-0326-0.
- Khanal, D., F. Zhang, Y. Song, H. Hau, A. Gautman, S. Yamaguchi, J. Uertz, S. Mills, A. Kondyurin, J. C. Knowles, et al. 2019. Biological impact of nanodiamond particles - label free high-resolution methods for nanotoxicity assessment. *Nanotoxicology* 13:1210–26. doi:10.1080/17435390.2019.1650970.
- Kitchin, K. T., E. Grulke, B. L. Robinette, and B. T. Castellon. 2014. Metabolomic effects in HepG2 cells exposed to four TiO₂ and two CeO₂ nanomaterials. *Environ Sci Nano* 1:466–77. doi:10.1039/C4EN00096J.
- Kmiec, Z. 2001. Co-operation of liver cells in health and disease. *Adv Anat Embryol Cell Biol* 161:1–151.
- Kojima, S., Y. Negishi, M. Tsukimoto, T. Takenouchi, H. Kitani, and K. Takeda. 2014. Purinergic signalling via P2X7 receptor mediates IL-1 β production in Kupffer cells exposed to silica nanoparticle. *Toxicology* 321:13–20. doi:10.1016/j.tox.2014.03.008.
- Kolosnjaj-Tabi, J., Y. Javed, L. Lartigue, J. Volatron, D. Elgrabli, I. Marangon, G. Pugliese, B. Caron, A. Figuerola, N. Luciani, et al. 2015. The one year fate of iron oxide coated gold nanoparticles in mice. *ACS Nano* 9:7925–39. doi:10.1021/acsnano.5b00042.
- Konduru, N., J. Keller, L. Ma-Hock, S. Gröters, R. Landsiedel, T. C. Donaghey, J. D. Brain, W. Wohlleben, and R. M. Molina. 2014. Biokinetics and effects of barium sulfate nanoparticles. *Part Fibre Toxicol* 11:55. doi:10.1186/s12989-014-0055-3.
- Kong, T., S. H. Zhang, J. L. Zhang, X. Q. Hao, F. Yang, C. Zhang, Z. J. Yang, M. Y. Zhang, and J. Wang. 2018. Acute and cumulative effects of unmodified 50-nm nano-ZnO on mice. *Biol Trace Elem Res* 185:124–34. doi:10.1007/s12011-017-1233-6.
- Kumar, R. P., and A. Abraham. 2016. PVP- coated naringenin nanoparticles for biomedical applications - *in vivo* toxicological evaluations. *Chem Biol Interact* 257:110–18. doi:10.1016/j.cbi.2016.07.012.
- Laux, P., J. Tentschert, C. Riebeling, A. Braeuning, O. Creutzenberg, A. Epp, V. Fessard, K. H. Haas, A. Haase, K. Hund-Rinke, et al. 2018. Nanomaterials: Certain aspects of application, risk assessment and risk communication. *Arch Toxicol* 92:121–41. doi:10.1007/s00204-017-2144-1.
- Lecave, J. M., U. Vicario-Pares, E. Bilbao, D. Gilliland, F. Mura, L. Dini, M. P. Cajaraville, and A. Orbea. 2018. Waterborne exposure of adult zebrafish to silver nanoparticles and to ionic silver results in differential silver accumulation and effects at cellular and molecular levels. *Sci Total Environ* 642:1209–20. doi:10.1016/j.scitotenv.2018.06.128.
- Lee, I. C., J. W. Ko, S. H. Park, N. R. Shin, I. S. Shin, C. Moon, J. H. Kim, H. C. Kim, and J. C. Kim. 2016. Comparative toxicity and biodistribution assessments in rats following subchronic oral exposure to copper nanoparticles and microparticles. *Part Fibre Toxicol* 13:56. doi:10.1186/s12989-016-0169-x.
- Lee, J. H., J. H. Sung, H. R. Ryu, K. S. Song, N. W. Song, H. M. Park, B. S. Shin, K. Ahn, M. Gulumian, E. M. Faustman, et al. 2018. Tissue distribution of gold and silver after subacute intravenous injection of co-administered gold and silver nanoparticles of similar sizes. *Arch Toxicol* 92:1393–405. doi:10.1007/s00204-018-2173-4.
- Lee, J. H., Y. S. Kim, K. S. Song, H. R. Ryu, J. H. Sung, H. M. Park, N. W. Song, B. S. Shin, D. Marshak, K. Ahn, et al. 2013. Bio-persistence of silver nanoparticles in tissues from Sprague-Dawley rats. *Part Fibre Toxicol* 10:36. doi:10.1186/1743-8977-10-36.
- Lekamge, S., A. F. Miranda, B. Pham, A. S. Ball, R. Shulka, and D. Nugegoda. 2019. The toxicity of non-aged and aged coated silver nanoparticles to the freshwater shrimp *Paratya australiensis*. *J Toxicol Env Health A* 82:1207–22. doi:10.1080/15287394.2019.1710887.
- Li, J., X. He, T. Yang, M. Li, C. Xu, and R. Yu. 2018a. Risk assessment of silica nanoparticles on liver injury in metabolic syndrome mice induced by fructose. *Sci Total Environ* 628:366–74. doi:10.1016/j.scitotenv.2018.02.047.
- Li, X., Z. Hu, J. Ma, X. Wang, Y. Zhang, W. Wang, and Z. Yuan. 2018b. The systematic evaluation of size-dependent toxicity and multi-time biodistribution of gold nanoparticles. *Colloids Surf B Biointerfaces* 167:260–66. doi:10.1016/j.colsurfb.2018.04.005.
- Li, Y., J. A. Bhalli, W. Ding, J. Yan, M. G. Pearce, R. Sadiq, C. K. Cunningham, M. Y. Jones, W. A. Monroe, P. C. Howard, et al. 2014. Cytotoxicity and genotoxicity assessment of silver nanoparticles in mouse. *Nanotoxicology* 8:36–45. doi:10.3109/17435390.2013.855827.
- Lim, J. P., G. H. Baeg, D. K. Srinivasan, S. T. Dheen, and B. H. Bay. 2017. Potential adverse effects of engineered nanomaterials commonly used in food on the miRNome. *Food Chem Toxicol* 109:771–79. doi:10.1016/j.fct.2017.07.030.
- Lingabathula, H., and N. Yellu. 2016. Cytotoxicity, oxidative stress, and inflammation in human Hep G2 liver epithelial cells following exposure to gold nanorods. *Toxicol Mech Method* 26:340–47. doi:10.3109/15376516.2016.1164268.

- Lipka, J., M. Semmler-Behnke, R. A. Sperling, A. Wenk, S. Takenaka, C. Schleh, T. Kissel, W. J. Parak, and K. G. Wolfgang. 2010. Bio-distribution of PEG-Modified gold nanoparticles following intratracheal instillation and intravenous injection. *Biomaterials* 31:6574–81. doi:10.1016/j.biomaterials.2010.05.009.
- Liu, L., M. Sun, Q. Li, H. Zhang, P. J. J. Alvarez, H. Liu, and W. Chen. 2014. Genotoxicity and cytotoxicity of cadmium sulfide nanomaterials to mice: Comparison between nanorods and nanodots. *Environ Eng Sci* 31:373–80. doi:10.1089/ees.2013.0417.
- Liu, Y., J. Ji, L. Ji, Y. Y. Li, B. W. Zhang, T. W. Tong, J. Yang, L. P. Ly, and G. Wu. 2019. Translocation of intranasal (i. n.) instillation of different sized cerium dioxide (CeO₂) particles: Potential adverse effects in mice. *J Toxicol Env Health A* 82:1069–75. doi:10.1080/15287394.2019.1686867.
- Louro, H., A. Tavares, N. Vital, P. M. Costa, E. Alverca, E. Zwart, W. H. de Jong, V. Fessard, J. Lavinha, and M. J. Silva. 2014. Integrated approach to the *in vivo* genotoxic effects of a titanium dioxide nanomaterial using LacZ plasmid-based transgenic mice. *Environ Mol Mutagen* 55:500–09. doi:10.1002/em.21864.
- Ma, T., L. Wang, T. Yang, G. Ma, and S. Wang. 2014. M-cell targeted polymeric lipid nanoparticles containing a toll-like receptor agonist to boost oral immunity. *Int J Pharmacol* 473:296–303. doi:10.1016/j.ijpharm.2014.06.052.
- MacParland, S. A., K. M. Tsoi, B. Ouyang, X. Z. Ma, J. Manuel, A. Fawaz, M. A. Ostrowski, B. A. Alman, A. Zilman, W. C. W. Chan, et al. 2017. Phenotype determines nanoparticle uptake by human macrophages from liver and blood. *ACS Nano* 11:2428–43. doi:10.1021/acsnano.6b06245.
- Magaye, R. R., X. Yue, B. Zou, H. Shi, H. Yu, K. Liu, X. Lin, J. Xu, C. Yang, A. Wu, et al. 2014. Acute toxicity of nickel nanoparticles in rats after intravenous injection. *Int J Nanomedicine* 9:1393–402. doi:10.2147/IJN.S56212.
- Mao, C., X. Chen, Q. Hua, G. Miao, and C. Lin. 2016. Acute toxicity and *in vivo* biodistribution of monodispersed mesoporous bioactive glass spheres in intravenously exposed mice. *Mater Sci Eng C* 58:682–91. doi:10.1016/j.msec.2015.09.002.
- Mendez, N., A. Liberman, J. Corbeil, C. Barback, R. Viveros, J. Wang, J. Wang-Rodriguez, S. L. Blair, R. Mattrey, D. Vera, et al. 2017. Assessment of *in vivo* systemic toxicity and biodistribution of iron-doped silica nanoshells. *Nanomedicine* 13:933–42. doi:10.1016/j.nano.2016.10.018.
- Mendonça, M. C. P., E. S. Soares, M. B. de Jesus, H. J. Ceragioli, S. P. Irazusta, A. G. Batista, M. A. R. Vinolo, M. R. M. Júnior, and M. A. da Cruz-Hofling. 2016. Reduced graphene oxide: Nanotoxicological profile in rats. *J Nanobiotechnology* 14:53. doi:10.1186/s12951-016-0206-9.
- Mirshafiee, V., B. Sun, C. H. Chang, Y. P. Liao, W. Jiang, J. Jiang, X. Liu, X. Wang, T. Xia, and A. E. Nel. 2018. Toxicological profiling of metal oxide nanoparticles in liver context reveals pyroptosis in Kupffer cells and macrophages versus apoptosis in hepatocytes. *ACS Nano* 12:3836–52. doi:10.1021/acsnano.8b01086.
- Mishra, A. R., J. Zheng, X. Tang, and P. L. Goering. 2016. Silver nanoparticle-induced autophagic-lysosomal disruption and NLRP3-inflammasome activation in HepG2 cells is size-dependent. *Toxicol Sci* 150:473–87. doi:10.1093/toxsci/kfw011.
- Mohamed, H. R. H., M. Welson, A. E. Yaseen, and A. El-Ghor. 2019. Induction of chromosomal and DNA damage and histological alterations by graphene oxide nanoparticles in Swiss mice. *Drug Chem Toxicol* 1:1–11. doi:10.1080/01480545.2019.1643876.
- Mohanan, P. V., C. S. Geetha, S. Syama, and H. K. Varma. 2014. Interfacing of dextran coated ferrite nanomaterials with cellular system and delayed hypersensitivity on guinea pigs. *Colloids Surf B Biointerfaces* 116:633–42. doi:10.1016/j.colsurfb.2013.10.033.
- Morishita, Y., Y. Yoshioka, Y. Takimura, Y. Shimizu, Y. Namba, N. Nojiri, T. Ishizaka, K. Takao, F. Yamashita, K. Takuma, et al. 2016. Distribution of silver nanoparticles to breast milk and their biological effects on breast-fed offspring mice. *ACS Nano* 10:8180–91. doi:10.1021/acsnano.6b01782.
- Natarajan, V., C. L. Wilson, S. L. Hayward, and S. Kidambi. 2015. Titanium dioxide nanoparticles trigger loss of function and perturbation of mitochondrial dynamics in primary hepatocytes. *PLoS ONE* 10:e0134541. doi:10.1371/journal.pone.0134541.
- Nguyen, K. C., Y. Zhang, J. Todd, K. Kittle, D. Patry, D. Caldwell, M. Lalande, S. Smith, D. Parks, M. Navarro, et al. 2019. Biodistribution and systemic effects in mice following intravenous administration of cadmium telluride quantum dot nanoparticles. *Chem Res Toxicol* 32:1491–503. doi:10.1021/acs.chemrestox.8b00397.
- Nguyen-Lefebvre, A. T., and A. Horuzsko. 2015. Kupffer cell metabolism and function. *J Enzymol Metab* 1:101.
- Oberdorster, G., A. Maynard, K. Donaldson, V. Castranova, J. Fitzpatrick, K. Ausman, J. Carter, B. Karn, W. Kreyling, D. Lai, et al. 2005. Principles for characterizing the potential human health effects from exposure to nanomaterials: Elements of a screening strategy. *Part Fibre Toxicol* 42:1–35.
- Park, E. J., G. H. Lee, C. Yoon, U. Jeong, Y. Kim, M. H. Cho, and D. W. Kim. 2016b. Biodistribution and toxicity of spherical aluminium oxide nanoparticles. *J Appl Toxicol* 36:424–33. doi:10.1002/jat.3233.
- Park, E. J., S. M. Kim, M. S. Kang, B. S. Lee, C. Yoon, U. Jeong, Y. Kim, G. H. Lee, D. W. Kim, and J. S. Kim. 2016a. A higher aspect ratio enhanced bioaccumulation and altered immune responses due to intravenously-injected aluminium oxide nanoparticles. *J Immunotoxicol* 13:439–48. doi:10.3109/1547691X.2015.1122116.
- Park, H. S., S. S. Shin, E. H. Meang, J. S. Hong, J. I. Park, S. H. Kim, S. B. Koh, S. Y. Lee, D. H. Jang, J. Y. Lee, et al. 2014. A 90-day study of subchronic oral toxicity of 20 nm, negatively charged zinc oxide nanoparticles in Sprague

- Dawley rats. *Int J Nanomedicine* 9:79–92. doi:10.2147/IJN.S57926.
- Patlolla, A. K., D. Hackett, and P. B. Tchounwou. 2015. Silver nanoparticle-induced oxidative stress-dependent toxicity in Sprague-Dawley rats. *Mol Cell Biochem* 399:257–68. doi:10.1007/s11010-014-2252-7.
- Pérez-Hernández, M., M. Moros, G. Stepien, P. Del Pino, S. Menao, M. de Las Heras, M. Arias, S. G. Mitchell, B. Pelaz, E. M. Gálvez, et al. 2017. Multiparametric analysis of anti-proliferative and apoptotic effects of gold nanoparticles on mouse and human primary and transformed cells, biodistribution and toxicity *in vivo*. *Part Fibre Toxicol* 14:41. doi:10.1186/s12989-017-0222-4.
- Ramachandran, R., C. Krishnaraj, V. K. A. Kumar, S. L. Harper, T. P. Kalaichelvan, and S. I. Yun. 2018. *In vivo* toxicity evaluation of biologically synthesized silver nanoparticles and gold nanoparticles on adult zebrafish: A comparative study. *Biotechnology* 8:441.
- Ramadi, K. B., Y. A. Mohamed, A. Al-Sbiei, S. Almarzooqi, G. Bashir, A. Al Dhanhani, D. Sarawathiamma, S. Qadri, J. Yasin, A. Nemmar, et al. 2016. Acute systemic exposure to silver-based nanoparticles induces hepatotoxicity and NLRP3-dependent inflammation. *Nanotoxicology* 10:1061–74. doi:10.3109/17435390.2016.1163743.
- Rawat, N., S. K. Sandhya, M. Eswaramoorthy, and G. Kaul. 2017. Comparative *in vivo* toxicity assessment places multi-walled carbon nanotubes at a higher level than mesoporous silica nanoparticles. *Toxicol Ind Health* 33:182–92. doi:10.1177/0748233715622307.
- Recordati, C., M. De Maglie, S. Bianchessi, S. Argenti, C. Cella, S. Mattiello, F. Cubadda, F. Aureli, M. D'Amato, A. Raggi, et al. 2015. Tissue distribution and acute toxicity of silver after single intravenous administration in mice: Nano-specific and size-dependent effects. *Part Fibre Toxicol* 13 (1):12. doi:10.1186/s12989-016-0124-x.
- Relier, C., M. Dubreuil, O. L. Garcia, E. Cordelli, J. Mejia, P. Eleuteri, F. Robidel, T. Loret, F. Pacchierotti, S. Lucas, et al. 2017. Study of TiO₂ P25 nanoparticles genotoxicity on lung, blood, and liver cells in lung overload and non-overload conditions after repeated respiratory exposure in rats. *Toxicol Sci* 156:527–37. doi:10.1093/toxsci/kfx006.
- Roberts, J. R., R. R. Mercer, A. B. Stefaniak, M. S. Seehra, U. K. Geddam, I. S. Chaudhuri, A. Kyrilidis, V. K. Kodali, T. Sager, A. Kenyon, et al. 2015. Evaluation of pulmonary and systemic toxicity following lung exposure to graphite nanoplates: A member of the graphene-based nanomaterial family. *Part Fibre Toxicol* 13 (1):34. doi:10.1186/s12989-016-0145-5.
- Rodrigues, D., M. Freitas, V. M. Costa, M. A. Lopez-Quintela, J. Rivas, P. Freitas, F. Carvalho, E. Fernandes, and P. Silva. 2017. Quantitative histochemistry for macrophage biodistribution on mice liver and spleen after the administration of a pharmacological-relevant dose of polyacrylic acid-coated iron oxide nanoparticles. *Nanotoxicology* 11:256–66. doi:10.1080/17435390.2017.1291865.
- Saber, A. T., A. Mortensen, J. Szarek, I. Kalevi Koponen, M. Levin, N. R. Jacobsen, M. E. Pozzebon, S. P. Mucelli, D. G. Rickerby, K. Kling, et al. 2015. Epoxy composite dusts with and without carbon nanotubes cause similar pulmonary responses, but differences in liver histology in mice following pulmonary deposition. *Part Fibre Toxicol* 13 (1):37. doi:10.1186/s12989-016-0148-2.
- Sadauskas, E., N. R. Jacobsen, G. Danscher, M. Stoltenberg, U. Vogel, A. Larsen, W. Kreyling, and H. Wallin. 2009. Bio-distribution of gold nanoparticles in mouse lung following intratracheal instillation. *Chem Cent J* 3:16. doi:10.1186/1752-153X-3-16.
- Sahu, S. C., S. Roy, J. Zheng, and J. Ihrle. 2016. Contribution of ionic silver to genotoxic potential of nanosilver in human liver HepG2 and colon Caco2 cells evaluated by the cytokinesis-block micronucleus assay. *J Appl Toxicol* 36:532–42. doi:10.1002/jat.3279.
- Sepehri, M., T. Sejersen, K. Qvortrup, C. M. Lerche, and J. Serup. 2017. Tattoo pigments are observed in the Kupffer cells of the liver indicating blood-borne distribution of tattoo ink. *Dermatology* 233:86–93. doi:10.1159/000468149.
- Shinohara, N., G. Zhang, Y. Oshima, T. Kobayashi, N. Imatanaka, M. Nakai, T. Sasaki, K. Kawaguchi, and M. Gamo. 2017. Kinetics and dissolution of intratracheally administered nickel oxide nanomaterials in rats. *Part Fibre Toxicol* 14:48. doi:10.1186/s12989-017-0229-x.
- Shrivastava, R., S. Raza, A. Yadav, P. Kushwaha, and S. J. S. Flora. 2014. Effects of sub-acute exposure to TiO₂, ZnO and Al₂O₃ nanoparticles on oxidative stress and histological changes in mouse liver and brain. *Drug Chem Toxicol* 37:336–47. doi:10.3109/01480545.2013.866134.
- Shukla, R. K., A. Kumar, N. V. S. Vallabani, A. K. Pandey, and A. Dhawan. 2014. Titanium dioxide nanoparticle-induced oxidative stress triggers DNA damage and hepatic injury in mice. *Nanomedicine* 9:1423–34. doi:10.2217/nnm.13.100.
- Silva, A. H., C. Locatelli, F. B. Filippin-Monteiro, P. Martin, N. J. Liptrott, B. G. Zanetti-Ramos, L. C. Benettie, E. M. Nazari, C. A. C. Albuquerque, A. A. Pasa, et al. 2016. Toxicity and inflammatory response in Swiss albino mice after intraperitoneal and oral administration of polyurethane nanoparticles. *Toxicol Lett* 246:17–27. doi:10.1016/j.toxlet.2016.01.018.
- Smulders, S., K. Luyts, G. Brabants, K. Van Landuyt, C. Kirschhock, E. Smolders, L. Golanski, J. Vanoirbeek, and P. H. M. Hoet. 2014. Toxicity of nanoparticles embedded in paints compared with pristine nanoparticles in mice. *Toxicol Sci* 141:132–40. doi:10.1093/toxsci/kfu112.
- Song, S. S., B. Y. Xia, J. Chen, J. Yang, X. Shen, S. J. Fan, M. Guo, Y. M. Sun, and X. D. Zhang. 2014. Two dimensional TiO₂ nanosheets: *In vivo* toxicity investigation. *RSC Adv* 4:42598–603. doi:10.1039/C4RA05953K.
- Sooklert, K., A. Wongjarupong, S. Cherdchom, N. Wongjarupong, D. Jindatip, Y. Phungnoi, R. Rojanathanes, and A. Sereemasun. 2019. Molecular and morphological evidence of hepatotoxicity after silver nanoparticle exposure: A systematic review, *in silico*, and ultrastructure investigation. *Toxicol Res* 35:257–70. doi:10.5487/TR.2019.35.3.257.

- Suzuki, T., N. Miura, R. Hojo, Y. Yanagiba, M. Suda, T. Hasegawa, M. Miyagawa, and R. S. Wang. 2016. Genotoxicity assessment of intravenously injected titanium dioxide nanoparticles in gpt delta transgenic mice. *Mutat Res* 802:30–37. doi:10.1016/j.mrgentox.2016.03.007.
- Talamini, L., M. B. Violatto, Q. Cai, M. P. Monopoli, K. Kantner, Z. Krpetić, A. Perez-Potti, J. Cookman, D. Garry, C. P. Silveira, et al. 2017. Influence of size and shape on the anatomical distribution of endotoxin-free gold nanoparticles. *ACS Nano* 11:5519–29. doi:10.1021/acsnano.7b00497.
- Tang, H., S. T. Yang, D. M. Ke, Y. F. Yang, J. H. Liu, X. Chen, H. Wang, and Y. Liu. 2017. Biological behaviours and chemical fates of Ag₂Se quantum dots *in vivo*: The effect of surface chemistry. *Toxicol Res* 6:693–704. doi:10.1039/C7TX00137A.
- Tee, J. K., L. Y. Ng, H. Y. Koh, D. T. Leong, and H. K. Ho. 2019. Titanium dioxide nanoparticles enhance leakiness and drug permeability in primary human hepatic sinusoidal endothelial cells. *Int J Mol Sci* 20:E35. doi:10.3390/ijms20010035.
- Thai, S. F., K. A. Wallace, C. P. Jones, H. Ren, E. Grulke, B. T. Castellon, J. Crooks, and K. T. Kitchin. 2016. Differential genomic effects of six different TiO₂ nanomaterials on human liver HepG2 cells. *J Biochem Mol Toxicol* 30:331–41. doi:10.1002/jbt.21798.
- Thakur, M., H. Gupta, D. Singh, I. R. Mohanty, U. Maheswari, G. Vanage, and D. S. Joshi. 2014. Histopathological and ultrastructural effects of nanoparticles on rat testis following 90 days (chronic study) of repeated oral administration. *J Nanobiotechnology* 12:42. doi:10.1186/s12951-014-0042-8.
- Thongkam, W., K. Gerloff, D. van Berlo, C. Albrecht, and R. P. F. Schins. 2017. Oxidant generation, DNA damage and cytotoxicity by a panel of engineered nanomaterials in three different human epithelial cell lines. *Mutagenesis* 32:105–15. doi:10.1093/mutage/gew056.
- Tiegs, G., and A. W. Lohse. 2010. Immune tolerance: What is unique about the liver. *J Autoimmun* 34 (1):1–6. doi:10.1016/j.jaut.2009.08.008.
- Tsoi, K. M., S. A. MacParland, X. Z. Ma, V. N. Spetzler, J. Echeverri, B. Ouyang, S. M. Fadel, E. A. Sykes, N. Goldaracena, J. M. Kathis, et al. 2016. Mechanism of hard-nanomaterial clearance by the liver. *Nat Mater* 15:1212–21. doi:10.1038/nmat4718.
- Valentini, X., P. Rugira, A. Frau, V. Tagliatti, R. Conotte, S. Laurent, J. M. Colet, and D. Nonclercq. 2019. Hepatic and renal toxicity induced by TiO₂ nanoparticles in rats: A morphological and metabonomic study. *Hindawi J Toxicol* 2019 (5767012):1–19. doi:10.1155/2019/5767012.
- Vance, M. E., T. Kuiken, E. P. Vejerano, S. P. McGinnis, M. F. Hochella, D. Rejeski, and M. S. Hull. 2015. Nanotechnology in the real world: Redeveloping the nanomaterial consumer products inventory. *Beilstein J Nanotechnol* 6:1769–80. doi:10.3762/bjnano.6.181.
- Vijayakumar, S., and B. Vaseeharan. 2018. Antibiofilm, anti cancer and ecotoxicity properties of collagen based ZnO nanoparticles. *Adv Powder Technol* 29:2331–45. doi:10.1016/j.appt.2018.06.013.
- Vranic, S., I. Gosens, N. R. Jacobsen, K. A. Jensen, B. Bokkers, A. Kermanizadeh, V. Stone, A. Baeza-Squiban, F. R. Cassee, L. Tran, et al. 2017. Impact of serum as a dispersion agent for *in vitro* and *in vivo* toxicological assessments of TiO₂ nanoparticles. *Arch Toxicol* 91:353–63. doi:10.1007/s00204-016-1673-3.
- Wallin, H., Z. O. Kyjovska, S. S. Poulsen, N. R. Jacobsen, A. T. Saber, S. Bengtson, P. Jackson, and U. Vogel. 2017. Surface modification does not influence the genotoxic and inflammatory effects of TiO₂ nanoparticles after pulmonary exposure by instillation in mice. *Mutagenesis* 32:47–57. doi:10.1093/mutage/gew046.
- Wang, C., Y. Bai, H. Li, R. Liao, J. Li, H. Zhang, X. Zhang, S. Zhang, S. T. Yang, and X. L. Chang. 2016. Surface modification-mediated biodistribution of ¹³C-fullerene C60 *in vivo*. *Part Fibre Toxicol* 13:14. doi:10.1186/s12989-016-0126-8.
- Wang, J., Y. Xie, L. Wang, J. Tang, J. Li, D. Kocaefe, Y. Kocaefe, Z. Zhang, Y. Li, and C. Chen. 2015. *In vivo* pharmacokinetic features and biodistribution of star and rod shaped gold nanoparticles by multispectral optoacoustic tomography. *RSC Adv* 5:7529–38. doi:10.1039/C4RA13228A.
- Wang, X., J. Gong, Z. Gui, T. Hu, and X. Xu. 2018b. Halloysite nanotubes-induced Al accumulation and oxidative damage in liver of mice after 30-day repeated oral administration. *Environ Toxicol* 33:623–30. doi:10.1002/tox.22543.
- Wang, X., W. Cheng, Q. Yang, H. Niu, Q. Liu, Y. Liu, M. Gao, M. Xu, A. Xu, S. Liu, et al. 2018a. Preliminary investigation on cytotoxicity of fluorinated polymer nanoparticles. *J Environ Sci* 69:217–26. doi:10.1016/j.jes.2017.10.014.
- Wang, Y., H. Zhao, D. Wang, M. Hao, C. Kong, X. Zhao, Y. Gao, J. Li, B. Liu, B. Yang, et al. 2019. Inhibition of autophagy promoted apoptosis and suppressed growth of hepatocellular carcinoma upon photothermal exposure. *J Biomed Nanotechnol* 15:813–21. doi:10.1166/jbn.2019.2714.
- Wang, Y., I. Zinonos, A. Zysk, V. Panagopoulos, G. Kaur, A. Santos, D. Losic, and A. Evdokiou. 2017. *In vivo* toxicological assessment of electrochemically engineered anodic alumina nanotubes: A study of biodistribution, subcutaneous implantation and intravenous injection. *J Mater Chem B* 5:2511–23. doi:10.1039/C7TB00222J.
- Wang, Y., Z. Chen, T. Ba, J. Pu, T. Chen, Y. Song, Y. Gu, Q. Qian, Y. Xu, K. Xiang, et al. 2013. Susceptibility of young and adult rats to the oral toxicity of titanium dioxide nanoparticles. *Small* 9:1742–52. doi:10.1002/smll.201201185.
- Wen, K. P., Y. C. Chen, C. H. Chuang, H. Y. Chang, C. Y. Lee, and N. H. Tai. 2015. Accumulation and toxicity of intravenously injected functionalized graphene oxide in mice. *J Appl Toxicol* 35:1211–18. doi:10.1002/jat.3187.
- Xie, J., W. Dong, R. Liu, Y. Wang, and Y. Li. 2018. Research on the hepatotoxicity mechanism of citrate-modified silver nanoparticles based on metabolomics and proteomics. *Nanotoxicology* 12:18–31. doi:10.1080/17435390.2017.1415389.

- Xue, Y., O. Chen, T. Ding, and J. Sun. 2014. SiO₂ nanoparticle-induced impairment of mitochondrial energy metabolism in hepatocytes directly and through a Kupffer cell-mediated pathway *in vitro*. *Int J Nanomedicine* 9:2891–903. doi:10.2147/IJN.S60661.
- Yang, L., H. Kuang, W. Zhang, H. Wei, and H. Xu. 2018a. Quantum dots cause acute systemic toxicity in lactating rats and growth restriction of offspring. *Nanoscale* 10:11564–77. doi:10.1039/C8NR01248B.
- Yang, P., H. Xu, Z. Zhang, L. Yang, H. Kuang, and Z. P. Aguilar. 2018b. Surface modification affect the bio-distribution and toxicity characteristics of iron oxide magnetic nanoparticles in rats. *IET Nanobiotechnol* 12:562–68. doi:10.1049/iet-nbt.2017.0152.
- Yang, Y., H. Bao, Q. Chai, Z. Wang, Z. Sun, C. Fu, Z. Liu, Z. Liu, X. Meng, and T. Liu. 2019. Toxicity, biodistribution and oxidative damage caused by zirconia nanoparticles after intravenous injection. *Int J Nanomedicine* 14:5175–86. doi:10.2147/IJN.S197565.
- Yang, Y., T. Zhao, T. Cheng, J. Shen, X. Liu, B. Yu, S. Lv, and H. Zhang. 2014. Hepatotoxicity induced by ZnO quantum dots in mice. *RSC Adv* 4:5642–48. doi:10.1039/c3ra46583g.
- Yu, S., F. Liu, C. Wang, J. Zhang, A. Zhu, L. Zou, A. Han, J. Li, X. Chang, and Y. Sun. 2018. Role of oxidative stress in liver toxicity induced by nickel oxide nanoparticles in rats. *Mol Med Rep* 17:3133–39. doi:10.3892/mmr.2017.8226.
- Yu, W. J., J. M. Son, J. Lee, S. H. Kim, I. C. Lee, H. S. Baek, I. S. Shin, C. Moon, S. H. Kim, and J. C. Kim. 2014. Effects of silver nanoparticles on pregnant dams and embryo-fetal development in rats. *Nanotoxicology* 8:85–91. doi:10.3109/17435390.2013.857734.
- Yun, J. W., S. H. Kim, J. R. You, W. H. Kim, J. J. Jang, S. K. Min, H. C. Kim, D. H. Chung, J. Jeong, B. C. Kang, et al. 2015. Comparative toxicity of silicon dioxide, silver and iron oxide nanoparticles after repeated oral administration to rats. *J Appl Toxicol* 35:681–93. doi:10.1002/jat.3125.
- Zane, A., C. McCracken, D. A. Knight, T. Young, A. D. Lutton, J. W. Olesik, W. J. Waldman, and P. K. Dutta. 2015. Uptake of bright fluorophore core-silica shell nanoparticles by biological systems. *Int J Nanomedicine* 10:1547–67. doi:10.2147/IJN.S76208.
- Zhang, J. Q., W. Zhou, S. S. Zhu, J. Lin, P. F. Wei, F. F. Li, P. P. Jin, H. Yao, Y. J. Zhang, Y. Hu, et al. 2017. Persistency of enlarged autolysosomes underscores nanoparticle-induced autophagy in hepatocytes. *Small* 13:1602876. doi:10.1002/smll.201602876.
- Zhang, X., J. Luan, W. Chen, J. Fan, Y. Nan, Y. Wang, Y. Liang, G. Meng, and D. Ju. 2018. Mesoporous silica nanoparticles induced hepatotoxicity via NLRP3 inflammasome activation and caspase-1-dependent pyroptosis. *Nanoscale* 10:9141–52. doi:10.1039/C8NR00554K.
- Zhang, Y., X. Xu, S. Zhu, J. Song, X. Yan, and S. Gao. 2016. Combined toxicity of Fe₃O₄ nanoparticles and cadmium chloride in mice. *Toxicol Res* 5:1309–17. doi:10.1039/C6TX00190D.
- Zhou, X., M. Dorn, J. Vogt, D. Spemann, W. Yu, Z. Mao, I. Estrela-Lopis, E. Donath, and C. Gao. 2014. A quantitative study of the intracellular concentration of graphene/noble metal nanoparticle composites and their cytotoxicity. *Nanoscale* 6:8535. doi:10.1039/C4NR01763C.
- Zhu, S., J. Zhang, L. Zhang, W. Ma, N. Man, Y. Liu, W. Zhou, J. Lin, P. Wei, P. Jin, et al. 2017. Inhibition of Kupffer cell autophagy abrogates nanoparticle-induced liver injury. *Adv Healthc Mater* 6:1601252. doi:10.1002/adhm.201601252.
- Zhu, S., X. Xu, R. Rong, B. Li, and X. Wang. 2016. Evaluation of zinc-doped magnetite nanoparticle toxicity in the liver and kidney of mice after sub-chronic intragastric administration. *Toxicol Res* 5:97–106. doi:10.1039/C5TX00292C.
- Zuo, D., Z. Duan, Y. Jia, T. Chu, Q. He, J. Yuan, W. Dai, Z. Li, L. Xing, and Y. Wu. 2016. Amphipathic silica nanoparticles induce cytotoxicity through oxidative stress mediated and p53 dependent apoptosis pathway in human liver cell line HL-7702 and rat liver cell line BRL-3A. *Colloids Surf B Biointerfaces* 145:232–40. doi:10.1016/j.colsurfb.2016.05.006.